**Federal University of Paraiba**

**Technology Center**

**CIVIL AND ENVIRONMENTAL ENGINEERING GRADUATE PROGRAM**

**– MASTERS –**

# SYNTHETIC ETTRINGITE IN SOLUTIONS CONTAINING CHLORIDE IONS

**Thiago Galvão Correia Lima**

**Dissertação de mestrado apresentado na Universidade Federal da Paraíba para aquisição do título de mestre**

**João Pessoa – Paraíba** **March 2022**

**Federal University of Paraiba**

**Technology Center**

**CIVIL AND ENVIRONMENTAL ENGINEERING GRADUATE PROGRAM**

**– MASTERS –**

# SYNTHETIC ETTRINGITE IN SOLUTIONS CONTAINING CHLORIDE IONS

**Dissertation submitted at the Civil and Environmental Engineering Graduate Program of the Federal University of Paraiba, as partial fulfillment for the acquisition of a Master's Degree.**

**Thiago Galvão Correia Lima**

**Supervisor: Prof. Dr. Sandro Marden Torres**

**João Pessoa – Paraíba** **March 2022**

**Catalogação na publicação**
**Seção de Catalogação e Classificação**

L732e Lima, Thiago Galvão Correia.
Etringita sintética em soluções contendo íons cloreto / Thiago Galvão Correia Lima. - João Pessoa, 2022.
59 f. : il.

Orientação: Sandro Marden Torres.
Dissertação (Mestrado) - UFPB/CT.

1. Etringita - Síntese. 2. Etringita - Concreto. 3. Cloro - Método sacarose. I. Torres, Sandro Marden. II. Título.

UFPB/BC CDU 549.057(043)

Elaborado por ANNA REGINA DA SILVA RIBEIRO - CRB-15/24

PPGECAM
Programa de Pós-Graduação
Engenharia Civil e Ambiental
UFPB Universidade Federal da Paraíba
Mestrado e Doutorado

*"ETRINGITA SINTÉTICA EM SOLUÇÕES CONTENDO ÍONS CLORETO"*

**THIAGO GALVÃO CORREIA LIMA**
**Dissertação aprovada em 30 de junho de 2022**

**Período Letivo: 2022.1**

**Prof. Dr. Sandro Marden Torres – UFPB**
**Orientador**

**Prof. Dr. Normando Perazzo Barbosa – UFPB**
**Examinador Interno**

**Prof. Dr. Romualdo Rodrigues Menezes – UFCG**
**Examinador Externo**

**João Pessoa/PB**
**2022**

“There is a way into my country from all the worlds,” said the Lamb; but as he spoke, his snowy white flushed into tawny gold and his size changed and he was Aslan himself, towering above them and scattering light from his mane”

(C. S. Lewis – The Chronicles of Narnia)

## ACKNOWLEDGEMENTS

To God, above all, my eternal gratitude.

My family: my parents Esdras and Germana and my two brothers, who are always by my side and who gave me opportunities, through education and prayers.

To professor Sandro for the collaboration and patience in passing on their knowledge for this work. His contribution was essential in increasing the level of research knowledge.

Thanks also to Professors Kelly and Edson, who kindly took some of their time to help me during the experimental sections of the FTIR and TGA. I would also like to thank the team at the Elizabeth Cimentos Chemical Analysis Laboratory for their assistance during the XRF test.

I would like to thank the Federal University of Paraíba for its collaboration over all these years and for encouraging my improvement.

To all the professors in our department who are sources of inspiration and for their support and attention to students.

To my friends and classmates, especially Fábio, for the shared experiences and who have always been companions in the main hours.

To the technicians and employees of the materials laboratory, for all the help in carrying out the tests for this work.

## RESUMO

A etringita, $Ca_6Al_2(SO_4)3(OH)12\cdot26H_2O$, é um mineral de estimada importância para a construção civil por ser um dos constituintes do concreto. Esse mineral pode ser encontrado na natureza de forma natural, bem como pode ser um dos resultantes da hidratação do cimento. Esse mineral é um dos primeiros minerais formado no endurecimento do cimento e sua formação durante o endurecimento é muito importante para o controle da pega e do tempo de uso do material até o seu endurecimento final, porém esse mineral pode ser formado tardiamente após o já endurecido concreto quando há falhas no controle tecnológico ou através de infiltração de sulfato por fontes externas levando a expansões indesejadas na sua estrutura. Devido a dificuldade de encontrar esse mineral de forma pura na natureza, foram desenvolvidos métodos de sintetização desse mineral que traz uma facilidade no seu desenvolvimento, bem como facilidade em substituir alguns elementos constituintes para os mais diversos fins. Este trabalho buscou analisar o papel do cloro em diferentes concentrações na estrutura da etringita, bem como a sua influencia na sua estabilização através do método de sacarose. A síntese da etringita foi bem sucedida e o cloro foi adsorvido na sua estrutura. Foi observado que quanto maior a concentração do íon cloro, maior era a estabilização da etringita e que a presença do íon cloro influenciou nos parâmetros da estrutura cristalina desse mineral. A partir da pesquisa apresentada e discutida nessa dissertação, podemos concluir que o cloro influencia na estabilização do mineral etringita.



**Palavras-chave:** Etringita, Cloro, Síntese, método sacarose.

## ABSTRACT

The ettringite, Ca6Al2(SO4)3(OH)12·26H2O, is a mineral of esteemed importance for civil construction because it is one of the constituents of concrete. This mineral can be naturally found in nature, as well as it can be one of those resulting from the hydration of cement. This mineral is one of the first minerals formed in cement hardening and its formation during hardening is very important for controlling the setting and the time of use of the material until its final hardening, but this mineral can be formed delayed after the already hardened concrete when there are failures in technological control or through the infiltration of sulfate by external sources leading to unwanted expansions in its structure. Due to the difficulty of finding this mineral in a pure form in nature, methods of synthesizing this mineral have been developed, which makes its development easier, as well as ease of substituting some constituent elements for the most diverse purposes. This work sought to analyze the role of chlorine at different concentrations in the structure of ettringite, as well as its influence on its stabilization through the saccharate method. The synthesis of ettringite was successful and chlorine was adsorbed on its structure. It was observed that the higher the concentration of chlorine ion, the greater the stabilization of ettringite and that the presence of chlorine ion influenced the parameters of the crystal structure of this mineral. From the research presented and discussed in this dissertation, we can conclude that chlorine influences the stabilization of the mineral ettringite.



**Keywords:** Ettringite, Chlorine, Synthesis, saccharate method.

## TABLE OF CONTENTS

## LIST OF SYMBOLS

| | |
|---|---|
| $C_{12}H_{22}O_{11}$ | Sucrose |
| $CaSO_4$ | Calcium Sulfate |
| ABNT | Brazilian Association of technical standards |
| $C_3A$ ou $3CaO.Al_2O_3$ | Tricalcium Aluminate |
| $CaSO_4.2H_2O$ | Calcium Sulfate Dihydrate (Gypsum) |
| $Ca_6[Al(OH)_6]_2(SO_4)_3.26H_2O$ | Ettringite |
| $C_4AF$ ou $Ca_2AlFeO_5$ | Tetracalcium ferroaluminate |
| $Ca(OH)_2$ | Calcium hydroxide |
| BSE | Backscattering electron |
| $Al(NO_3)3.9HO$ | Aluminum Nitrate Nonahydrate |
| NaCl | Sodium chloride |
| DTA | Differential Thermal Analysis |
| DSC | Differential scanning calorimetry |
| EDS | Energy dispersive spectroscopy |
| MEV | Scanning Electron Microscopy |
| IV-FT | Fourier-transform infrared spectroscopy |
| DRX | X-ray diffraction |
| SE | Secondary electron |
| FRX | X-ray fluorescence |
| TGA | Thermogravimetric analysis |
| $\lambda$ | X-ray wavelength |
| d | Characteristic distance between the planes of the crystal structure |
| $\theta$ | Diffraction angle |
| KBr | Potassium Bromide |
| $H_2O$ | Water |
| $CO_2$ | Carbon dioxide |

| | |
|---|---|
| $SiO_2$, | Silicon dioxide |
| $Fe_2O_3$ | Iron oxide |
| MgO | Magnesium oxide |
| $Na_2O$ | Sodium Oxide |
| $Al_2O_3$ | Aluminum Oxide |
| CaO | Calcium oxide |
| $SO_3$ | Sulfur Trioxide |
| $CaCO_3$ | Calcium carbonate |

## LIST OF FIGURES

## LISTA DE TABELAS

# 1. INTRODUCTION

## 1.1 Organization of the Contents

This work was divided into four chapters: introduction, literature review, materials and methods, results and discussions and conclusions.

Chapter 1 – The introduction is intended to provide the initial ideas about the topic. It is through it that more elaborate information about the context of the topic and a brief description of the subject will be provided. Then, the reasons for the study will be discussed along with the relevance of the topic in the context of civil construction pathologies. Finally, we will be discussed what are the objectives pursued with the realization of these studies.

Chapter 2 – Materials and Methods is intended to present the materials that were used for the synthesis of ettringite with chlorine, together with the experimental design of the synthesis. Furthermore, the characterization techniques used are briefly presented.

Chapter 3 – Results and Discussions present the results of the characterization of synthetic ettringite through the techniques and the discussions about the collected data.

Chapter 4 – Conclusions summarize the main ideas drawn from the studies carried out. Furthermore, it presents recommendations for future work in the investigation of the role of chlorine as a constituent of ettringite.

## 1.2 Initial considerations

The study of pathology in concrete structures appears in the field of Civil Engineering as a need to repair the various existing defects, even with the advent of the Implementation of Quality Management Systems - ISO 9001 in construction companies, this occurs due to poor execution of the works, design flaws, imperfection of materials, or even the three coexisting cases.

The ever-accelerated growth of civil construction, in some countries and times, has provoked the need for innovations that have brought, in themselves, the implicit acceptance of greater risks. Along with these risks, came the inevitable involuntary failures and cases of malpractice, which caused unsatisfactory performance in some structures according to each purpose for which they were proposed. Although much still needs to be studied, as it is a very vast and interdisciplinary field, knowledge related to the pathology of structures has advanced over time due to the lessons emanating from the day-to-day constructions and, mainly, due to

the justification of scientific achievement achieved by research carried out. (SOUZA AND RIPPER, 1998).

An analysis of the origin of these pathologies is of paramount importance in construction processes, regardless of whether their origin comes from the project, its construction process, or how it is used. No less important is the knowledge of the mechanisms and the forms of concrete deterioration, to promote restoration or structural reinforcement according to the pathological need.

Several cracking mechanisms, whether by mechanical, electrochemical, or geochemical phenomena, are responsible for unsatisfactory performance in several structures. However, among these various processes that can cause excessive cracking, excessive cracking, drying shrinkage, sulfate attack and corrosion of steel by chloride attack stand out. Among these various failures that can cause unsatisfactory performance, there is the formation of ettringite in already hardened concrete. An example of this pathology can be represented below.

Figure 1. Pathology related to the expansion of ettringite in sulfate attack on a concrete prism

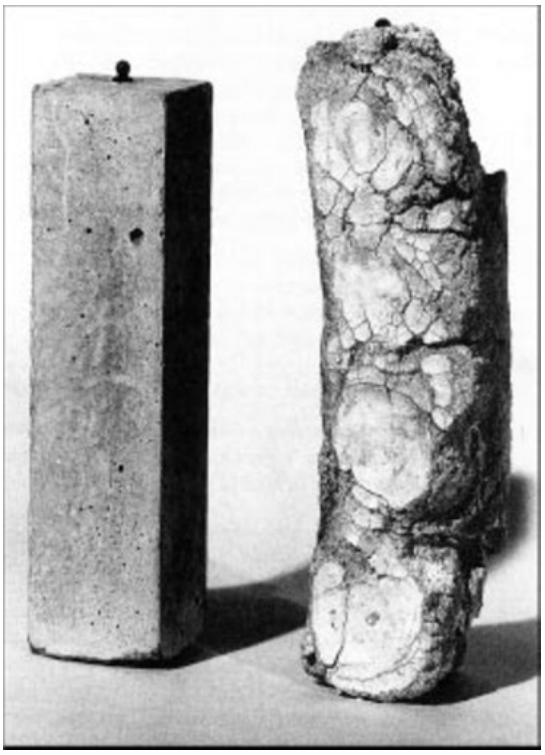

Source: Telford (1989)

Ettringite is a rare mineral in nature, but a common product that occurs during the hydration of Portland cement. Its formation is directly related to microstructural expansion, but its formation is not always related to structural collapse. In addition, (BAQUERIZO et al.,

2015) cite that ettringite is also the main hydration product of special binders, such as calcium sulfate cement and calcium aluminate cement mixed with calcium sulfates. When its formation is homogeneous and during the plastic state of the concrete, its formation does not cause any considerable cracking and is known as primary ettringite (COLLEPARDI, 2003). Its formation at an early age is associated with the use of added sulfates to prevent the rapid hardening of the concrete. Its formation has a fundamental role in the control and configuration of the cement and its formation is responsible for the "handling" of the cement. (MONTEIRO; P. MEHTA, 2005)

The formation of ettringite at ages after the complete hardening of the concrete, due to the delayed formation of ettringite, can cause degradation of concrete structures. This mineral formation can be inhibited when the heat of hydration of the concrete has values above 65º, therefore when the source of sulfate is internal and its formation is inhibited during the plastic phase of the cement, the crystallization of ettringite is later known as secondary ettringite or late.

Other causes of secondary ettringite formation are sulfate infiltration by external sources, such as soil, contaminated water, and stored materials, among others. Soils that have more than 3000 ppm of sulfates are problematic, so the formation of ettringite is inevitable and needs special attention (SARGENT, 2015). Sulfate attack causing expansive ettringite in concrete exposed to aggressive soil is probably the most familiar type reported and, for a time, was the only serious pathology reported (BENSTED; RBROUGH; PAGE, 2007). The crystals formed in the pores and voids after the concrete is hardened, due to its increase in volume, end up generating internal tensions, thus destroying the concrete body. The expansion is considerable, the transformation of 1 mol of calcium hydroxide to gypsum generates an increase in solid volume from 33.2 $cm^3$ to 74.3 $cm^3$, therefore, more than double, since the transformation of hydrated calcium aluminate or gypsum to ettringite also generates a greater than double increase in volume (BENSTED; RBROUGH; PAGE, 2007).

The ettringite has the formula $Ca_6[Al(OH)_6]_2(SO_4)_3.26H_2O$, it can be found in nature as a mineral formed from the weathering of rocks. in the shape of hexagonal prisms or needles. Below is an example of a sample of ettringite taken from nature.

Figure 2. Photograph of an ettringite crystal

Source: Lavinsky (2020)

In cement, ettringite is normally needle-shaped in its initial reaction phase. Sometimes this mineral occupies the voids and pores within the cured concrete (YUAN et al., 2021) and within the phases of the already hydrated and cured concrete, it has the least dense phase. The precipitation of ettringite in Portland cement, generated mainly in needles, has two ways of being precipitated.

The first form is the product of crystalline precipitation that can be as hydrated calcium monosulfoaluminate or hydrated calcium trisulfoaluminate, also known as ettringite from the hydration reaction between $C_3A$ and calcium sulfate (CaSO4) (MONTEIRO; P MEHTA, 2005). The second form, depending on the concentration of dissolved aluminate and sulfate, can be formed with $C_3A$ and $C_4AF$. The crystallization of ettringite is rapid and, normally, the first hydrate to crystallize in the formation of concrete, it is also responsible for the initial development of cement hardening (MORANVILLE-REGOURD; KAMALI-BERNARD, 2019).

One of the ways to obtain ettringite is through a selective extraction, but it is an arduous way to obtain it. In order to facilitate the study of this mineral, several authors have developed ways to synthesize it and one of the first scientists to develop this method were the scientists I. Odler and Abdul-Maula who in 1984 developed five synthesis methods, however, among these, two of them were plus an adaptation of the first three synthesizing methods by changing the mixes. These scientists aimed to quantitatively determine this mineral in hydrated cement pastes and as a way to facilitate its study, they developed methods to synthesize it. Their five synthesis methods were based on mixtures of tricalcium aluminate ($3CaO.Al_2O_3$) with gypsum ($CaSO_4.2H_2O$). Another method was from the mixture of $Al2(SO_4)_3.18H_2O$ with $Ca(OH)_2$

(ODLER; ABDUL-MAULA, 1984). Some of these methods were replicated in several other studies, such as the one by Warren and Reardon in 1994, which aimed to study the solubility of ettringite at 25ºC (WARREN; REARDON, 1994), and the one by Ávarez-Ayuso and Nugteren in 2005, which aimed to study the reuse of residues for the synthesis of ettringite (ÁLVAREZ-AYUSO; NUGTEREN, 2005).

Other scientists perfected these methods by introducing sucrose as a way to inhibit the absorption of carbon dioxide. Such as Pollmann; Kuzel; Wenda (1989). This method was used for this purpose in this research using such knowledge, but the results in this context were not satisfactory as will be discussed later in this dissertation. This method is known as the sucrose method due to the introduction of this item to the desired synthesis mixture and is a form already widespread in the scientific environment. The other importance of using sucrose is that it facilitates the formation of ettringite in compounds that contain gypsum (MARTÍNEZ-RAMÍREZ et al., 2016). The sugar binds to the calcium oxide increasing the solubility of this compound in water. When starting the formation of ettringite, calcium oxide joins for its formation and has no difficulty separating from sucrose, since its bond with this compound has a weak bond. Therefore, sucrose plays an important role in the synthesis of the sample.

## 1.3 Justification and relevance of the topic

There are two common ways that chlorine is present in concrete. The first are ions that associate with the sample already hardened by external means. A very common example is the direct contact of seawater, rich in sodium chloride, with the concrete piece. The other way is through chloride ions incorporated during mixing when the sample is still fluid, this way is known as internal chlorides. Ions incorporated into the mixture is already a method practiced for a long time, with the main purpose of accelerating the setting in the mixture, mainly in low temperature situations.

When analyzing research related to the implementation of chlorine in the mixture, the object of research is usually as a set accelerator. However, a few studies do not address this issue and envision the effect of chlorine in delaying the formation of late ettringite. These studies were conducted mainly in South Africa and concluded that at low concentrations of chlorides, there is an instability of monosulfates generating the formation of late ettringite (EKOLU; THOMAS; HOOTON, 2006). However, the situation changes when there is a higher concentration of chloride ions leading to a suppression of expansion due to late ettringite. It is

aware that chlorine is adsorbed on the ettringite structure and its integration with the structure influences the interaction with water molecules (HOU et al., 2018).

Cement is the second most consumed material on the planet, second only to water. It is an important binder and its use is directly related to the development of a nation. ettringite is one of the constituents of this material and has its proper role. Therefore, the studies developed here are of great importance in exploring the influence of chlorine in the interaction with the structure of ettringite. In addition, the studies seek to explore a topic that is so current and little-explored: studies in this area are concentrated in this millennium and it is very difficult to find subjects that address this theme. Little has been discussed and studied about this subject and the synthesis of ettringite.

## 1.4 Objectives

### *1.4.1 Main Objective*

To analyze the role of chlorine at different concentrations in the structure of ettringite, as well as its influence on its stabilization using the sucrose method.

### *1.4.2 Secondary Objectives*

Confirm the analogous phases of synthesis using the sucrose method through the experiments;

To verify the influence of the variation of the chlorine concentration in the stabilization of the ettringite;

Evaluate the reaction products obtained through XRD, XRF, IV-FT, DTA/DTG and SEM.

# 2 MATERIALS AND METHODS

This chapter talks about the materials used in the research, as well as all the details of the procedures for the synthesis procedure. In addition, all the characterization techniques used for the development of the research will be described.

## 2.1 Precursor materials

For the synthesis of ettringite under the laboratory conditions that will be described later, four reagents were used, namely: $Ca(OH)_2$, $Al(NO_3)_3.9H_2O$, $CaSO_4.2H_2O$ and NaCl. The decision to use these materials is based on the fact that they have a good purity index and have good solubility in water at room temperature.

In addition to the reagents, sucrose from refined sugar cane was used in the reactions. Refined sugar has 99.9% sucrose which has the formula $C_{12}H_{22}O_{11}$. Its main function is in the food industry, but it is also used in civil construction as a setting retarder in concrete by reducing the solubility of hydrated compounds in cement. It was used in fine powder form, it has good solubility (200 g/dL at 25ºC).

The calcium hydroxide used was supplied by the manufacturer Dinâmica Química Contemporânea Ltda. It is a colorless crystal or, as supplied, in the form of a white powder. The manufacturer guaranteed a purity of 95% with 3% of its impurity of $CaCO_3$. Of the precursor materials used, it is the one with the worst solubility (0.16 g/dL at 25ºC) and has the interesting characteristic of retrograde solubility that decreases solubility as the water temperature increases. To characterize the samples, the material was kept in an oven at 100ºC, then crushed and filtered into particles no larger than 75 μm. The resulting powder was subjected to XRD. Rietveld structural refinement was performed to refine the parameters of the cell unit along with the atomic positions, the result is shown below in Figure 3.

Figure 3. Diffractogram of calcium hydroxide used

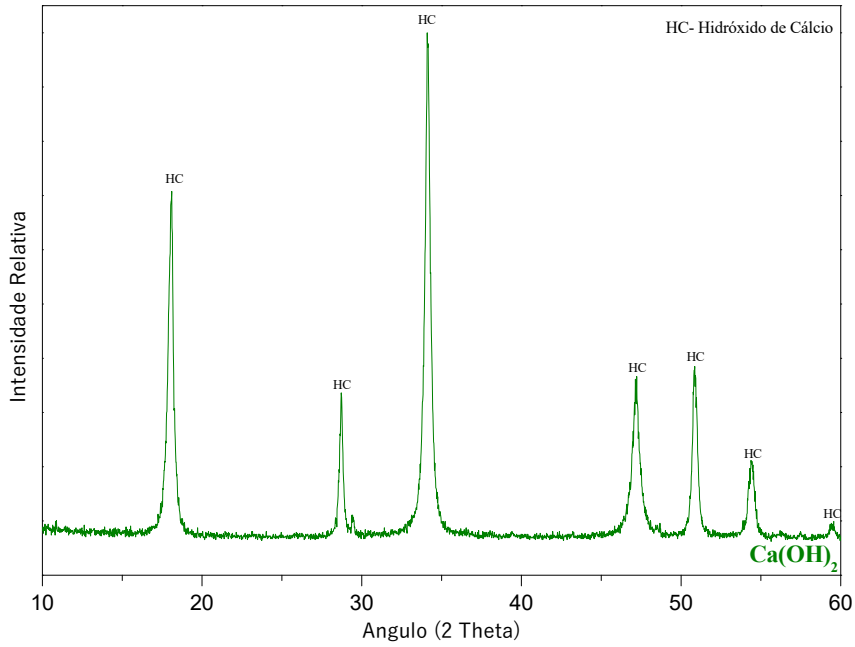


Source: Own authorship.

Aluminum nitrate is a white salt that is very soluble in water (73.9 g/dL at 25ºC). It was also supplied by the company Dinâmica Química Contemporânea Ltda in the form of small pearls. The manufacturer has guaranteed a purity of 98.5% in the material. It is widely used in the consumer goods industry as antiperspirants, in the construction industry as corrosion inhibitors, and in extractive industries it is used in uranium extraction and petroleum refinement. The powder used was subjected to Rietveld structural refinement and the result is shown below in figure 4.

Figure 4. Diffractogram of aluminum nitrate used

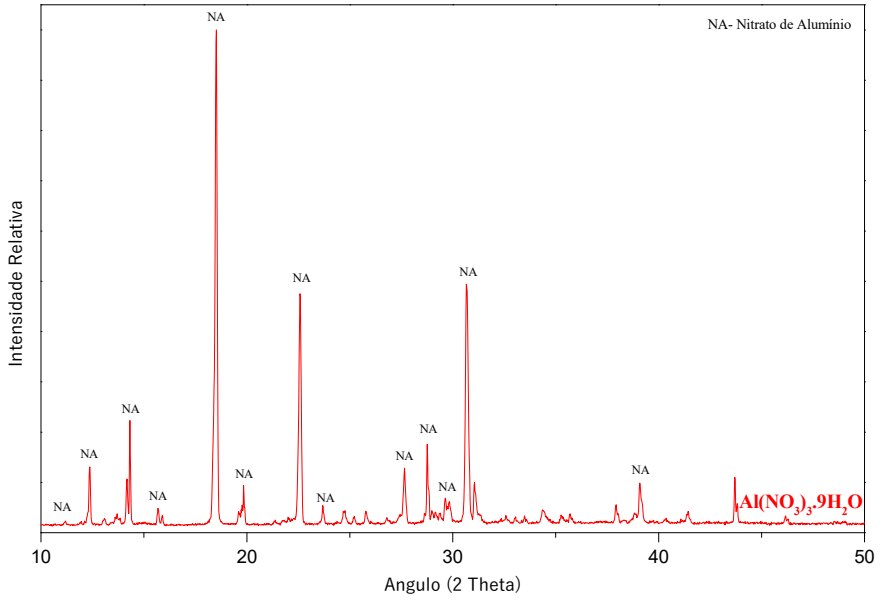


Source: Own authorship.

Calcium sulfate dihydrate is an inorganic salt that is poorly soluble in water (0.24 g/dL at 25ºC), is also known as gypsum and is widely used in industries, especially in civil construction. It was produced by the company Vetec Química Fina Ltda. The manufacturer has guaranteed a purity of 98.0% in the material. and delivered in the form of a white powder and a very fine granulometry. The powder used was subjected to Rietveld structural refinement and the result is shown below in figure 5.

Figure 5. Diffractogram of calcium sulfate dihydrate used

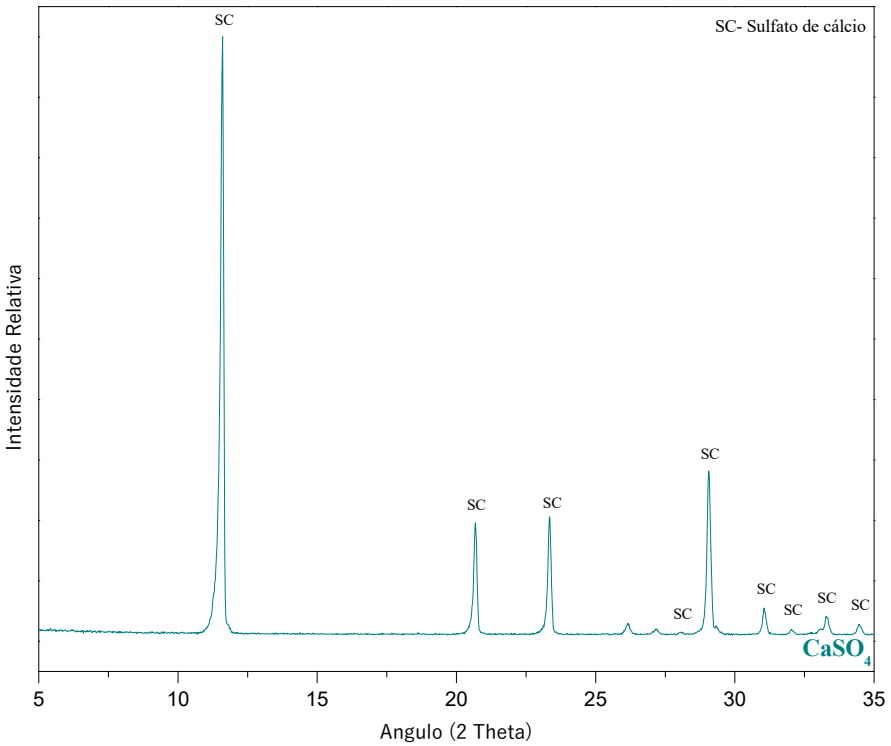

Source: Own authorship.

Sodium chloride, popularly known as table salt, is a very soluble salt (74.5 g/dL at 25ºC) and was supplied by the company F Maia Industria e Comercio Ltda in the form of a white powder with fine granulometry. The manufacturer has guaranteed a purity of 99.0% in the material. The powder used was subjected to Rietveld structural refinement and the result is shown below in figure 6.

Figure 6. Diffractogram of the sodium chloride used

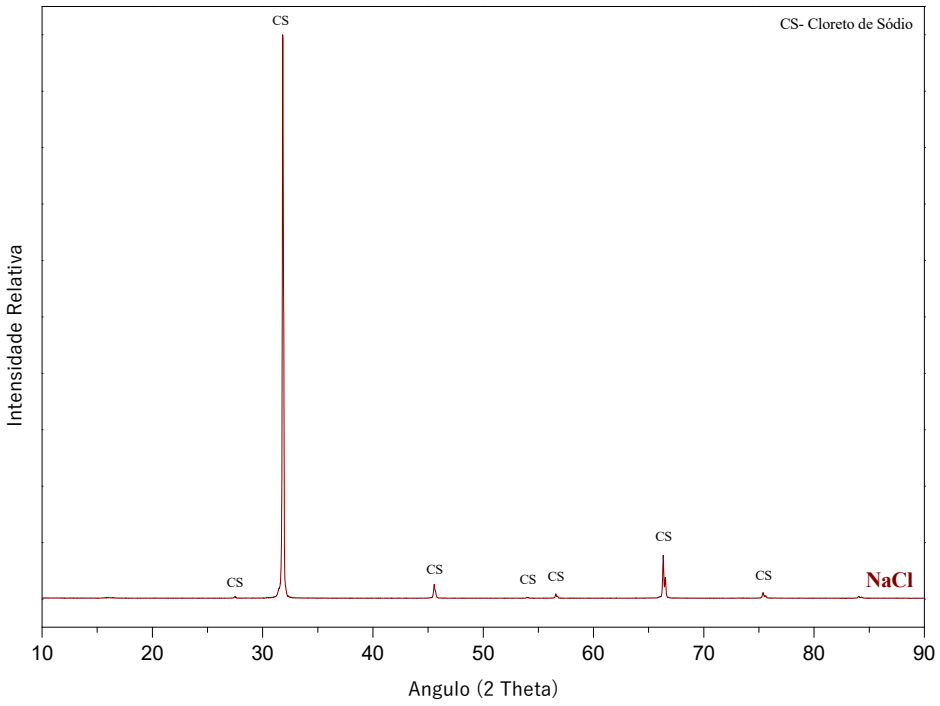


Source: Own authorship.

## 2.2 Synthesis Method

Powder samples from the synthesis of ettringite were created based on the precipitation method called the “saccharate method” (POELLMANN et al., 1993). Before starting the experiment, it was necessary to determine the exact amount of each precursor to produce approximately 200 grams of each ettringite sample, a sufficient amount to carry out all the tests proposed in topic 3.3. With the help of the Solver tool of the Microsoft Excel program, the exact amount and concentration of each proposed solution were found. After calculations and quantity science, the synthesis method was prepared in the following steps:

The first step was to prepare the sucrose solution. 30% refined sugar with 99.8% purity was added to a solution of deionized water. After good hand mixing and ensuring that all sucrose was dissolved, the solution was separated into a plastic container.

The next step was the preparation of the elements. The sucrose solution was gently added to each of the chemical elements for their dissolution to help in the homogeneity of the mixture. These solutions were manually shaken for 2 minutes, closed and kept for a while until all elements were mixed.

Then the calcium hydroxide solution was added together with the aluminum nitrate solution, the calcium sulfate dihydrate solution was also added together, and the sodium chloride solution was also added. Soon after, the resulting solution was gently mixed in search of the most homogeneous solution possible. This resulting solution was separated into a plastic container, then closed and sealed and stored.

This process was repeated for the nine samples that can be divided into three distinct groups of sodium chloride concentration. These samples were separated at room temperature for the determined time of each one and as the determined synthesis time arrived, the samples were opened and the following steps were continued. These samples can be summarized in Table 1.

Table 1. Concentration and reaction time of each sample

| Sample | chlorine concentration | Synthesis time |
|---|---|---|
| **1D 05C** | 0.5% | 1 day |
| **1D 10C** | 1.0% | 1 day |
| **1D 20C** | 2.0% | 1 day |
| **3D 05C** | 0.5% | 3 days |
| **3D 10C** | 1.0% | 3 days |
| **3D 20C** | 2.0% | 3 days |
| **7D 05C** | 0.5% | 7 days |
| **7D 10C** | 1.0% | 7 days |
| **7D 20C** | 2.0% | 7 days |

Source: Own authorship.

In the next step the samples were filtered. A simple filtration method was adopted. In this process, deionized water was added to the ettringite solution as a way to remove all sucrose used in the process, the raw materials of the reaction and as a way to avoid the partial dissolution of ettringite at low pH.

After the filtering process, the samples were placed directly in the oven at 50oC for five days until all free water remaining in the sample was evaporated. The final result was a solid, rigid and white sample.

The last step was the sieving process. Part of these hardened samples were ground in a porcelain mill. This ball mill has a container with a capacity of 1 liter, made of porcelain, accompanied by a lid with a rubber gasket in a rotation of 45 rpm for 30 minutes. After this process, the samples were sieved according to NBR 7217 procedure recommendations in 200 and 315 mesh sieves. The resulting samples were saved for the various proposed characterization tests.

These processes were summarized in Figure 3 below in flowchart format with some observations.

Figure 7. Summary of synthetic ettringite production procedures

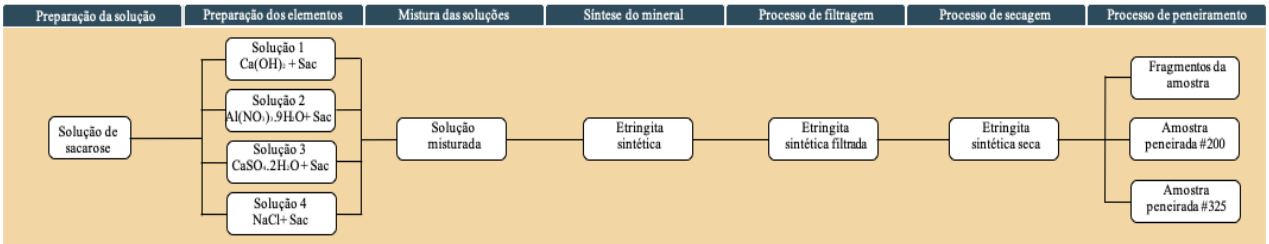


| | | | | | | |
|---|---|---|---|---|---|---|
| A solução de sacarose foi preparada utilizando o método de Poellmann (1993) e separada em um depósito de plástico | A solução de sacarose foi gentimente derramada sobre cada um dos elementos químicos e misturados até sua total dissolução. | As soluções 1, 2, 3 e 4 foram gentimente derramadas uma sobre a outra e misturadas manualmente até se ter uma solução homogênea. A solução resultante foi separada em um depósito de plástico e fechada. | A solução resultante foi separada a temperatura ambiente até o tempo estipulado (1, 3 ou 7 dias). | Após o tempo estipulado para cada uma das amostras, o recipiente de plástico foi aberto. Após isso foi feito o processo de filtração simples com adição de água deionizada até a retirada de toda sacarose. | A etringita foi colocada em uma estufa a 50° C até que a água livre remanescente fosse evaporado. | As amostras endurecidas foram trituradas em um moinho de bolas cerâmico e peneiradas em telas de mesh 200 e 315. |

Source: Own authorship.

## 2.3 Characterization techniques

This topic will address the main characterization techniques used for the results of this research, as well as important information about the parameters of the tests.

### *2.3.1 Scanning Electron Microscopy*

SEM has the potential to produce images by scanning from a focus of an electron beam on a surface (YANG, 2008a). In a typical SEM, electrons are thermionically emitted from a tungsten or lanthanum hexaboride ($LaB_6$) cathode (filament) and accelerated through an anode. Tungsten is typically used as it has the highest melting point and lowest vapor pressure, allowing it to be heated for electron emission. The electron beam, which normally has an energy

ranging from a few hundred eV to 100keV, is focused by one or two condensing lenses into a beam with a very fine focal point, ranging in size from 0.4 to 0 .5 nm. This beam travels through two scanning coils and two deflection plates in the microscope frame.

As the primary electron beam interacts with the material, the electrons lose energy by scattering and absorbing in a volume known as the drop-shaped interaction volume. This volume extends from 100nm to around 5 μm into the surface of the material. The size of this volume depends on several factors, among which the main ones are the atomic number of the atoms of the material to be pumped by the beam and the energy of the electron beam. The figure below shows how this process takes place.

Figure 8. Zone of interaction between electrons and atoms of any surface.

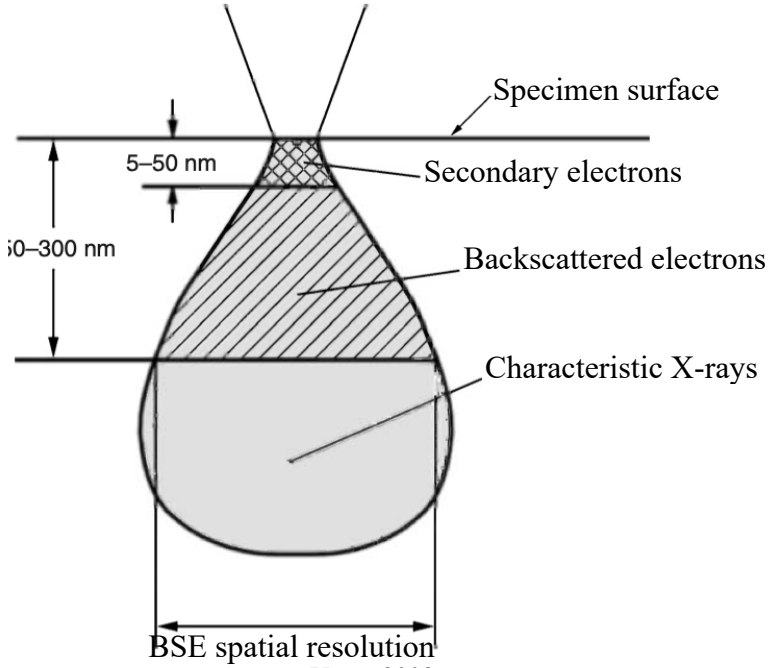


Source: Yang, 2008

From the moment that there is contact between the electron beam and the surface of the material, secondary electrons (SE), backscattered electrons (BSE) and characteristic x-rays are emitted. The signal is collected by the microscope detector and is used for observation. The SE is the product of an inelastic scattering, while the BSE is a product of an elastic scattering, because of this, images formed from SE tend to have a better spatial resolution than the one generated from BSE, thus, Secondary electrons are more suitable for topographical contrast of the surface area of the material, whereas backscattered electrons are more suitable for generating contrast of material composition (YANG, 2008). In the images of a BSE product,

those darker regions are the regions that have lighter elements, whereas the lighter regions have heavier elements.

For this research, the samples were crushed and sieved in sieve No 200, after which each sample was embedded in carbon tape. After doing this process for each sample, they were coated with gold.

The SEM analysis consisted of making images with magnification of 10000 and 25000 to detect the visual characteristics of the minerals generated by the synthesis of each one. The FEI Quanta 450 scanning electron microscope was used for this step. The samples were taken in a high vacuum with a filament voltage of 15 kV and a working distance of 5.3 mm.

### *2.3.2 X-Ray Diffraction*

X-ray diffraction is the most accurate method for determining the crystal structure of a material, this phenomenon has the potential to generate an interference pattern in the waves of an X-ray beam from the interaction between the X-ray beam and the structure. crystalline material. This technique is more recommended for determining the atomic and molecular structure of the crystalline material, because the X-ray beams, when falling on some crystalline material, diffract in a specific direction, therefore, for each type of crystalline material, there is a pattern of XRD curve. specific.

XRD is based on constructive interference at specific angles generated from the scattering of light through a periodic matrix with long-range order (CHATTERJEE, 2001), so the detector moves through a circular motion around the sample, as shown in the image below. , counting the X-ray intensity by recording the number for each angle.

Figure 9. Graphic representation of the XRD device

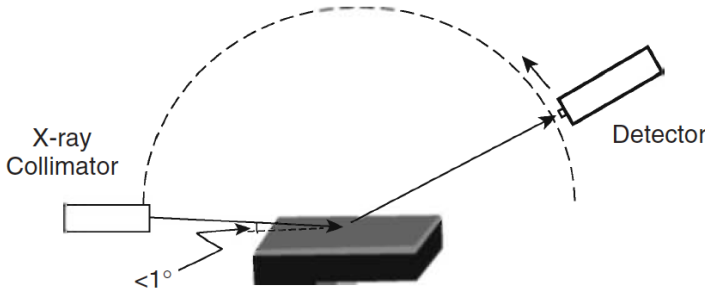


Source: Yang, 2008

The angles can be calculated through Bragg's law that created the correlation between the X-ray wavelength (λ), characteristic distance between the planes of the crystal structure (d) and the diffraction angle (θ) through the following formula.

$$n\lambda = 2d \sin\theta \qquad \text{Equation 1}$$

XRD analyzes were performed using a Bruker D2 Phaser diffractometer, using CuKα radiation at a rate of 1º/min, in a 2θ range from 5º to 70º and a preset measurement time of 1.2 seconds.

### *2.3.3 Chemical Analysis by X-Ray Fluorescence*

Chemical analysis by X-Ray Fluorescence provides fundamental data for the characterization of materials through the quantification and identification of the chemical elements present in the sample, although it does not allow a complete evaluation of the mineralogical composition. The most usual determinations are in the form of the most stable oxides of the chemical elements present in the compositions of the constituent phases of the compounds formed after the reaction process. The XRF analyzes the chemical elements of the samples by detecting the characteristic rays emitted by the samples, as shown in the image below, after pumping the X-rays (YANG, 2008c).

Figure 10. Characteristic excitation produced by pumping X-rays

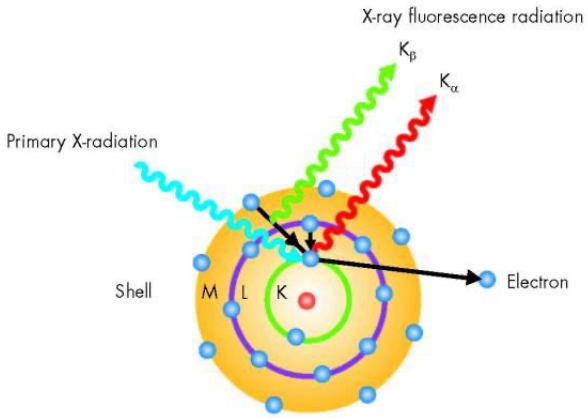


Source: Fischer (2020)

Chemical analysis was performed on the PANalytical Axios Max spectrometer at Elizabeth Cimentos' Chemical Analysis Laboratory. The samples were prepared in the form of

plates from the mixture between the sample, lithium metaborate and ammonium iodide in their proper proportions, after which they were placed in a platinum crucible and subjected to 1000ºC for 15 minutes to form the plates. Through the XRF, the percentages of the compounds in terms of oxide mass (%).

### *2.3.4 Fourier transform infrared spectroscopy*

When a molecule is excited by infrared radiation, they move to a higher energy state, but not all bonds in a molecule have the potential to absorb energy in the infrared, only bonds that have a dipole moment are able to absorb energy. infrared radiation (L. PAVIA; M. LAMPMAN, 2016). Because each bond produces a specific intrinsic frequency and because two identical bonds in two different compounds have a slight difference in their environment, therefore, infrared absorption in two molecules of different structures will have different infrared absorption patterns. Due to this characteristic, the infrared spectrum will have its individuality for each molecule.

The Fourier Transform Infrared Spectrometer (FT-IV) has the ability to produce a trace of the optical path, thus producing a pattern called an interferogram. This interferogram contains all the frequencies that form the infrared spectrum in the form of waves and a mathematical operation known as the Fourier transform manages to separate the individual frequencies contained in this interferogram (L. PAVIA; M. LAMPMAN, 2016).

The IV-FT samples were prepared from the mixture of very finely ground ettringite with potassium bromide (KBr) powder under high pressure, the final result was in the form of a very thin and translucent pellet. The mixture was given in 1 mg of ettringite powder for 100 mg of KBr. This mixture was made taking care to mix well and leave the mixture as homogeneous as possible. The IV-FT experiment was performed on an IRTracer-100 Shimadzu spectrometer at the partner laboratory of synthetic thin films at UFPB.

### *2.3.5 Thermal Analysis*

Thermal analysis is nothing more than a group of techniques in which a sample is monitored in relation to time or temperature while the temperature of the sample, in a specified atmosphere, is programmed (ICTA, 1991). These techniques allow analyzing the state of the sample such as temperature, mass, volume, among others, thus allowing the analysis of

chemical composition of the material, crystalline structures of the sample, transition heat, heat capacity, among other material properties (OZAWA, 2000). ).

There are a number of characterization techniques that use thermal analysis, among the most used we can mention Thermogravimetric Analysis (TGA), Differential Thermal Analysis (DTA) and Scanning Scanning Calorimetry (DSC). TGA measures the amount and rate of change in weight of a material as a function of temperature or time in an atmosphere of some gas or in a vacuum. In DTA, a reference is used and the sample and reference material are heated in an oven. The difference between the sample temperature and the reference material temperature is recorded during programmed heating and cooling cycles. DSC is a technique for measuring the thermal behavior of substances to make a connection between temperature and some of their specific physical properties. (ABRAHAM et al., 2018).

The thermal analysis experiments were performed on a simultaneous type thermal analyzer of the TA Instruments brand and the SDT 650 model in the partner laboratory of synthetic thin films at UFPB. About 7 mg of each ettringite sample was placed in an alumina crucible and exposed to thermal variation from 25 °C to 1010 °C, at a constant heating rate of 10 °C/min and in an inert atmosphere (argon) that was used to prevent possible reactions with the released gases.

# 3 RESULTS AND DISCUSSION

## 3.1 Visual Assessment

The visual aspects of the samples were performed in two moments: right after the filtering process and after drying for 5 days in an oven at 50ºC. It is interesting to observe that right after the filtering process they all had the same pasty appearance of milky white color. Below is a comparison by varying the concentration of chlorine in the synthesis of ettringite.

Figure 11. Visual aspects of ettringite samples after filtering process

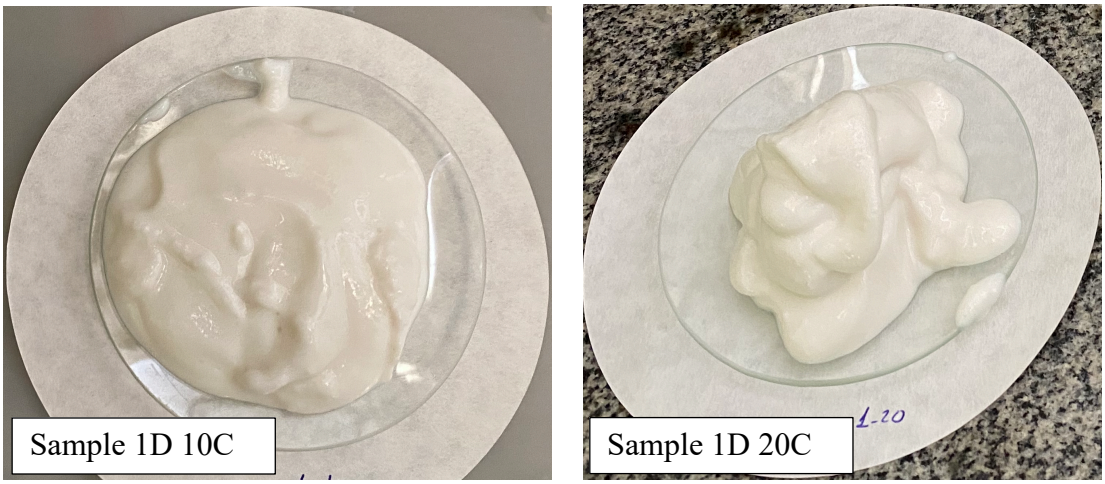


Source: Own authorship.

After the drying process, the common characteristics remained for all of them, as they all had the same visual property of being milky white and of being rigid, porous and easily disintegrated by tension. Below is a comparison by varying the number of days of ettringite synthesis.

Figure 12. Visual aspects of ettringite samples after drying process


Source: Own authorship.

These results show that, visually, the synthesis of all samples was successful in the formation of ettringite since the optical property of the samples is within the optical characteristics of ettringite which is opaque and milky white ("Handbook of Mineralogy," 2020). Another factor to explain these characteristics is a small presence of gypsum that has visual characteristics similar to those of ettringite.

### 3.2 Chemical Analysis by X-Ray Fluorescence

Chemical analysis by X-ray fluorescence has the importance of showing the chemical composition of ettringite syntheses in terms of oxide mass percentage. This data can be briefly shown in table two below. A large amount of fire loss was observed for all samples. This loss is mainly associated with the levels of H2O and CO2 in the sample. The chemical composition of ettringite ($Ca_6[Al(OH)_6]_2(SO_4)_3.26H_2O$) has a proportion of water mass, equivalent to 37% for all mineral, and most of the sample corresponds to ettringite as can be seen. see the XRD and thermal analysis results in topic 3.4 and 3.5 respectively. The rest of the loss on fire can be explained through the results of XRD and IV-FT, it was also possible to observe that the samples have calcite, aragonite and gypsum together with ettringite. Calcite, as an example, turns into calcium oxide and carbon dioxide, so all these materials have either water or carbon dioxide in their composition, so all these materials were responsible for the high value of loss on fire.

Table 2. XRF results in terms of oxide mass percentage for each synthesized sample

| Sample | Fire Loss (%) | $SiO_2$ (%) | $Al_2O_3$ (%) | $Fe_2O_3$ (%) | CaO (%) | MgO (%) | $SO_3$ (%) | $Na_2O$ (%) |
|---|---|---|---|---|---|---|---|---|
| **1D 05C** | 47,55 | 0,39 | 7,88 | 0,08 | 29,33 | 0,27 | 14,45 | 0,03 |
| **1D 10C** | 48,25 | 0,21 | 7,87 | 0,07 | 29,4 | 0,28 | 13,91 | 0,03 |
| **1D 20C** | 48,76 | 0,24 | 7,59 | 0,06 | 29,09 | 0,3 | 13,93 | 0,02 |
| **3D 05C** | 47,45 | 0,21 | 7,96 | 0,07 | 29,44 | 0,31 | 14,62 | 0,02 |
| **3D 10C** | 45,26 | 0,18 | 8,31 | 0,05 | 30,96 | 0,28 | 14,99 | 0,03 |
| **3D 20C** | 45,49 | 0,26 | 8,18 | 0,06 | 30,67 | 0,3 | 15,08 | 0,03 |
| **7D 05C** | 35,13 | 0,27 | 9,58 | 0,04 | 36,67 | 0,36 | 17,84 | 0,03 |
| **7D 10C** | 47,21 | 0,23 | 8,11 | 0,05 | 32,42 | 0,29 | 11,24 | 0,06 |
| **7D 20C** | 51,34 | 0,42 | 7,31 | 0,1 | 31,75 | 0,33 | 8,04 | 0,07 |

Source: Own authorship.

Small impurities were observed in the samples, this includes: $SiO_2$, $Fe_2O_3$, MgO and $Na_2O$. Their sum varies from 0.54% for the purest synthesis (3D 10C sample) to 0.92% for the synthesis with more impurities (7D 20C sample). As expected, the main values found are for aluminum oxide, calcium oxide and sulfur oxide, constituents of the main minerals in the samples, which are ettringite, gypsum and calcite.

### 3.3 Fourier transform infrared spectroscopy

The IV-FT experiment was used in order to identify the chemical groups present in each of the samples and testify that the ettringite synthesis was successful. Likewise, it is also possible to make a comparison between the groups of samples and verify the participation of chlorine as a constituent of ettringite.

The spectrogram of all samples is very similar and similar peaks stand out. All samples showed the spectrogram of sulfate, carbonate, aluminate as well as structural water and free water in their composition. These groups can be identified in Figure 13 below through the arrow indications.

Figure 13. IV-FT of all ettringite syntheses with indications of chemical groups through arrows

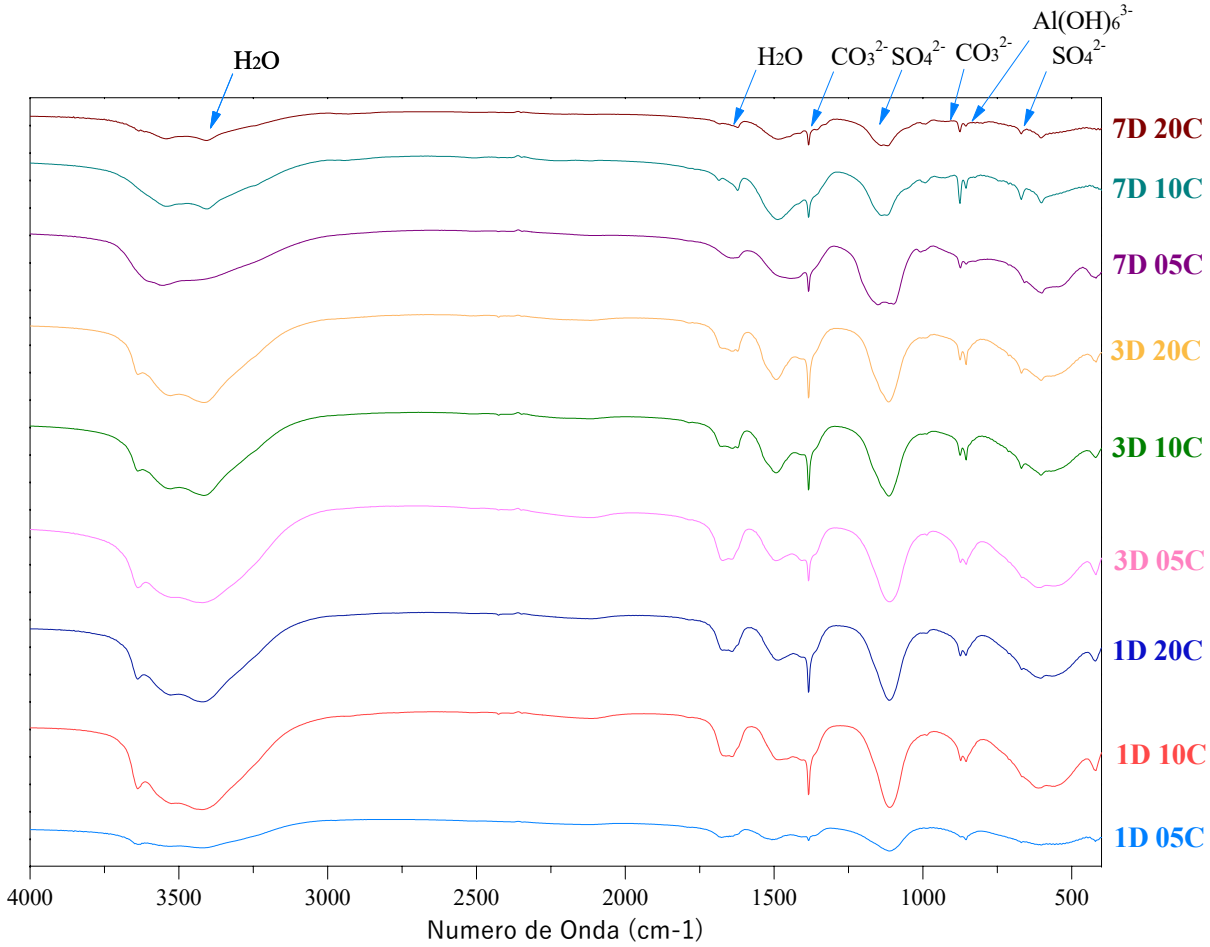


Source: Own authorship.

The bonds observed between 3200 and 3600 cm-1 in all samples are associated with the vibration of hydroxyl groups in water molecules chemically bound to ettringite. Likewise, the bonds observed between 1600 and 1700 are associated with water as well (NAKAMOTO, 2008). This idea is in tune with the character of the sample that has water in its composition and is hydrophilic.

In figures 14, 15 and 16 are the 1, 3 and 7 day spectrograms for 0.5%, 1.0% and 2.0% chlorine in the ettringite composition respectively. They will be presented between the period from 400 cm-1 to 1300 cm-1, this is justified by the fact that it is in this region where the peaks of the ettringite constituents are concentrated and to avoid undesirable peaks such as free water and bound water that do not will be important to the discussions.

Figure 14. IV-FT for 0.5% chlorine in the synthesis of ettringite with indications of chemical groups through arrows

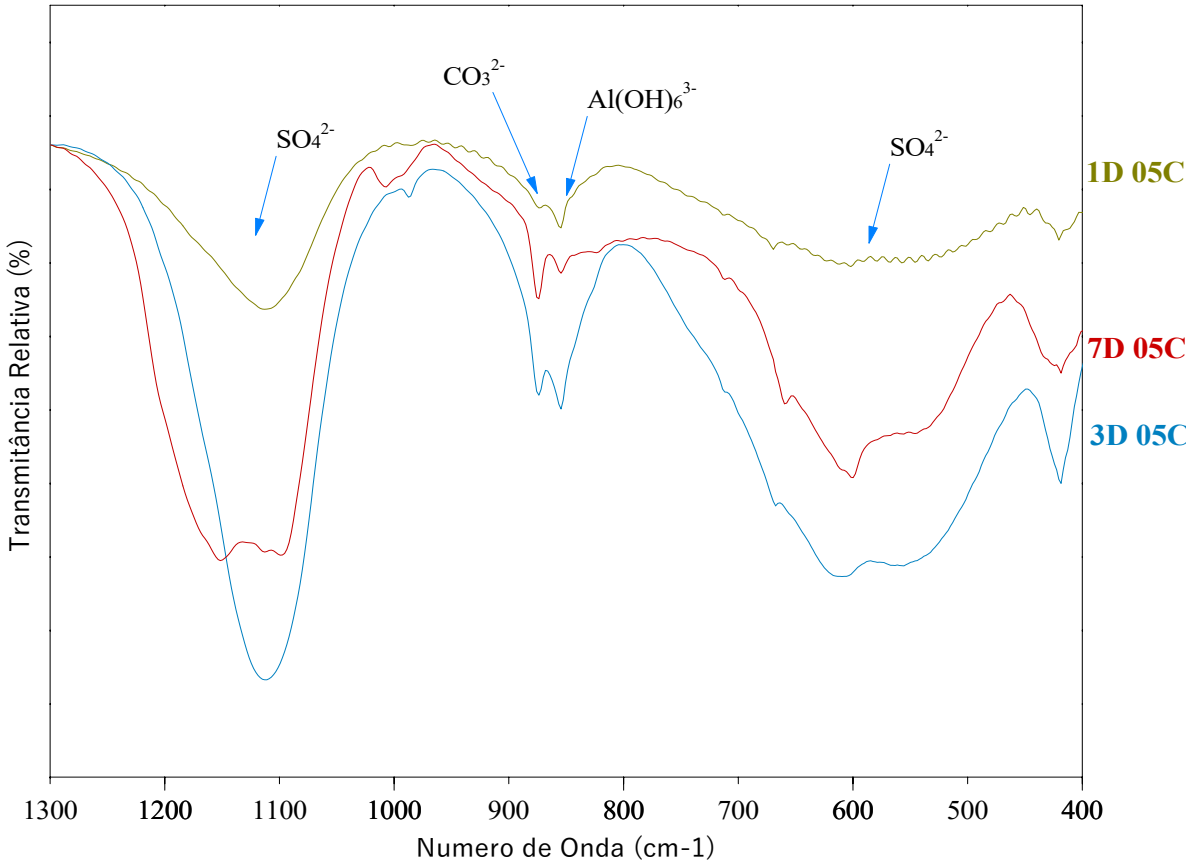


Source: Own authorship.

The presence of carbonate is not expected, because within the structure of ettringite, as seen in chapter 1 of this dissertation, this constituent does not exist, but it was identified in all samples at wavelengths 1400 and 900. When analyzing the curves of XRD we verified that calcite and aragonite minerals exist for all samples and these minerals have carbonate in their composition. Therefore, a plausible explanation for the undesired presence of carbonate is due to the formation of these two minerals during the synthesis of ettringite when the air, which has carbon dioxide in its constitution, is not excluded from the reaction environment. This carbon dioxide reacts with calcium from the calcium hydroxide precursor, used in the reaction,

generating these undesirable minerals. Another form of contamination is through the use of precursor materials with impurities. About 3% of calcium carbonate was supplied together with the calcium hydroxide used as a precursor of the synthesis.

Figure 15. I V-FT for 1.0% chlorine in the synthesis of ettringite with indications of chemical groups through arrows

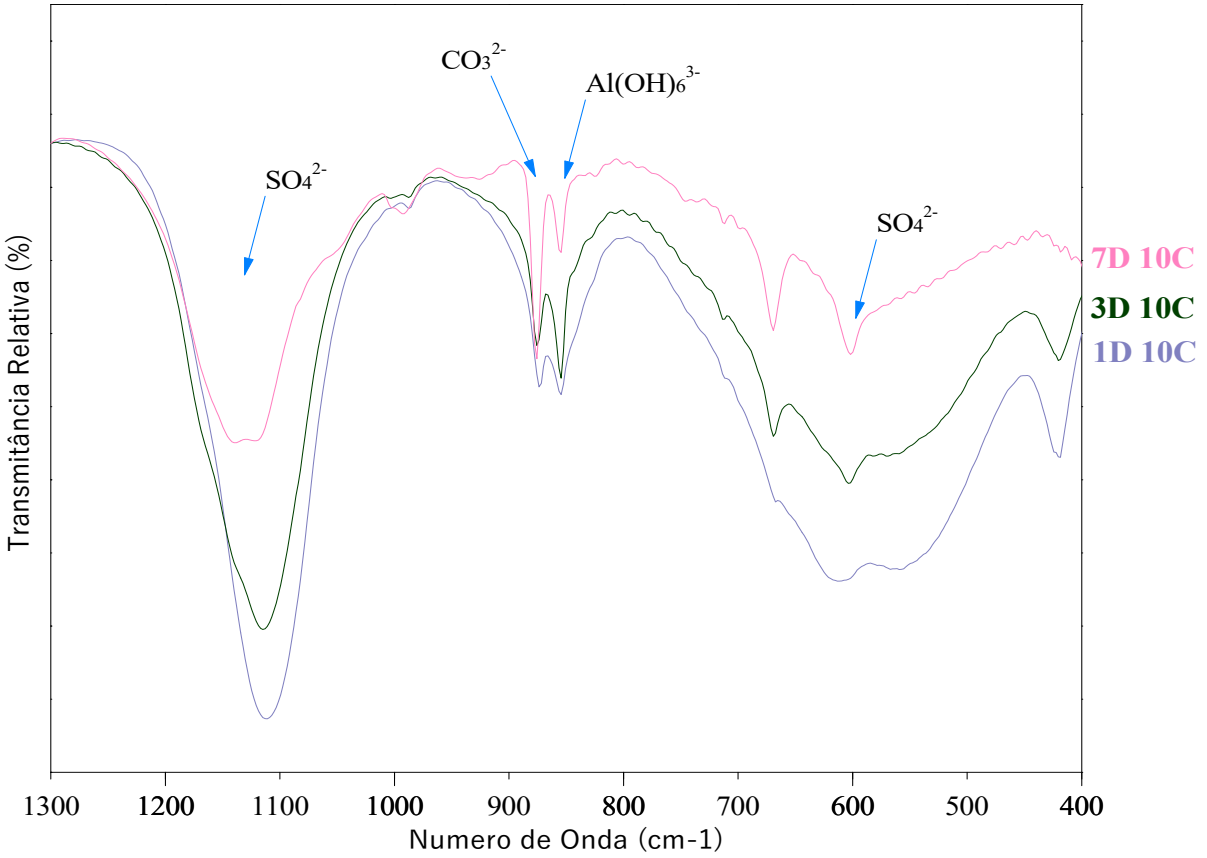


Source: Own authorship.

Furthermore, the presence of peaks in the region of 1100 and 1150 cm-1 indicates the presence of sulfates (NAKAMOTO, 2008; NORMAN et al., 2013). On the other hand, peaks between 820 and 870 cm-1 indicate the presence of aluminum in the composition of ettringite (NORMAN et al., 2013). Therefore, the presence of these peaks indicates that the phases formed are actually from ettringite.

Another important point observed is that the carbonate, as it forms, ends up destroying the sulfate present in the ettringite. This decrease is seen in Figure 15, while the sulfate peaks are well developed for one day of reaction, they decrease for seven days of reaction. The inverse circumstance is observed for carbonate, while for one day of reaction its peak is poorly developed, for seven days this peak is well-formed.

It is also interesting to observe that the aluminum peak is smaller in the 7-day samples when compared to the 1 and 3-day samples, this shows a deterioration of the ettringite when the aluminum is no longer octahedral. This observation is in agreement with the XRD data in topic 4.4 of this dissertation, which shows a lower amount of ettringite in the samples after seven days of reaction. This destruction of ettringite may be related to the concentration of chlorine in the sample that prevents the development of ettringite.

Figure 16. IV-FT for 2.0% chlorine in the synthesis of ettringite with indications of chemical groups through arrows

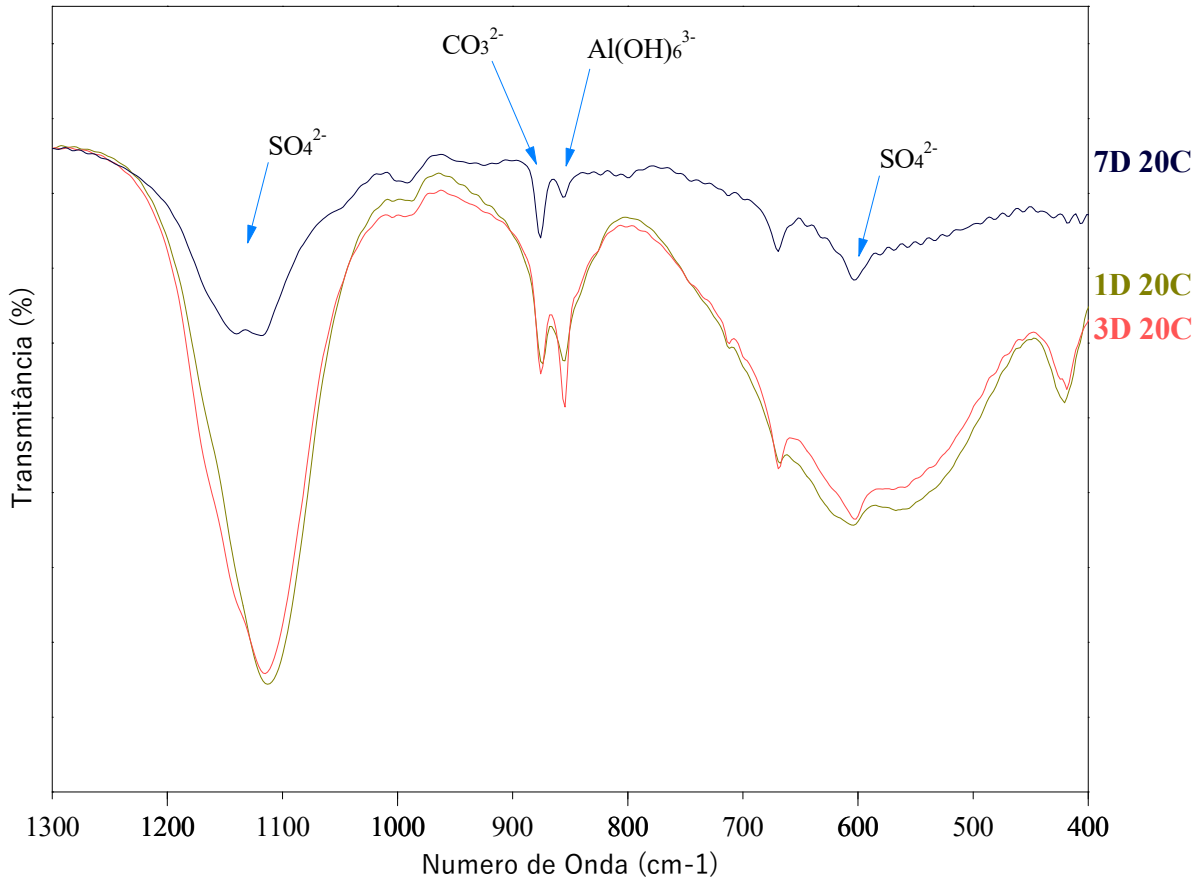


Source: Own authorship.

## 3.4 X-Ray Diffraction

A satisfactory resolution was obtained from a Bruker D2 Phaser diffractometer. In addition, Rietveld structural refinement was performed in the Topas program also provided by the company Bruker to refine the parameters of the cell unit along with the atomic positions. The results obtained, refined and calculated can be seen from figure 17 to figure 19. The diffractograms were organized as follows: samples with 0.5% chlorine in the synthesis are

shown in image 17, while samples with 1.0 % chlorine in the synthesis are shown in image 18, finally, samples with 2.0% chlorine in the synthesis are shown in image 19.

Figure 17. XRD for 0.5% chlorine in ettringite synthesis with mineral indications

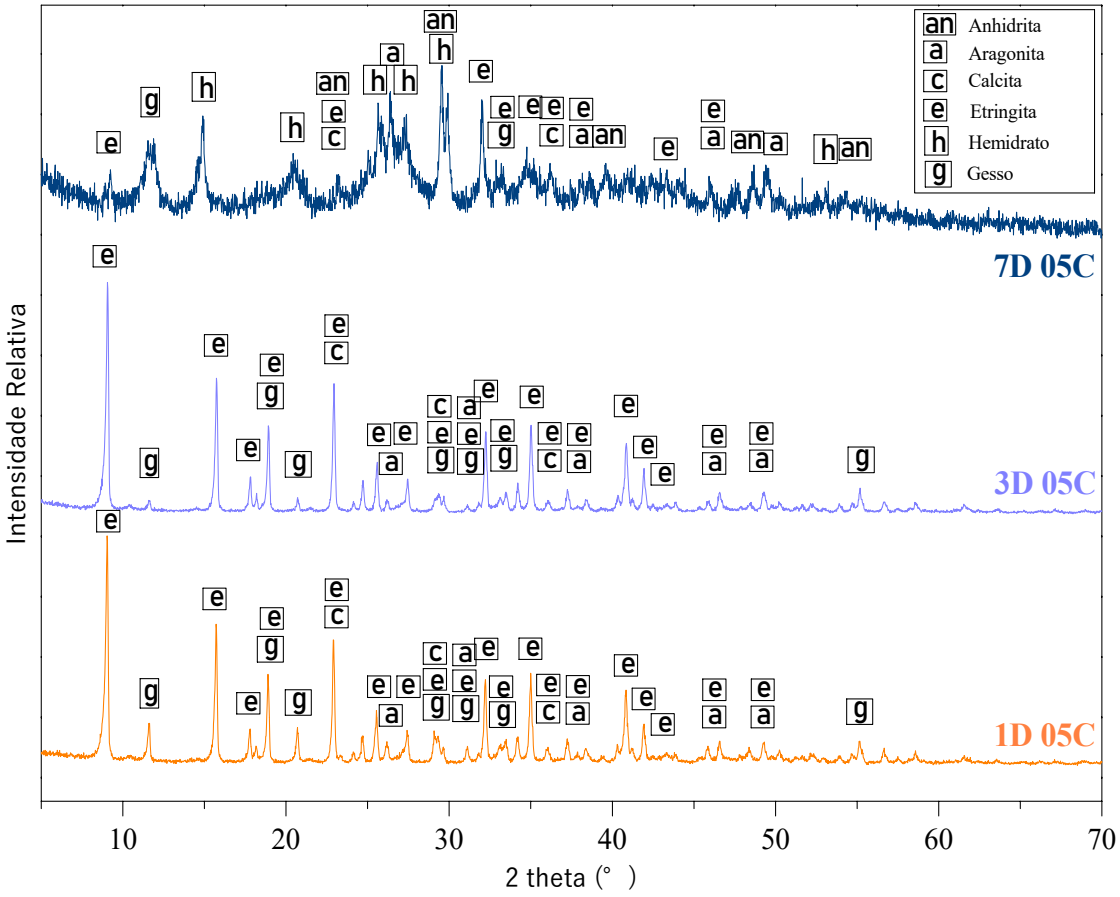


Source: Own authorship.

It is possible to observe that, in general, the samples are crystalline, except the 0.5% chlorine sample for 7 days of the experiment, which has a semi-crystalline nature. In general, all samples presented ettringite, aragonite and calcite in their composition.

Regarding the identified phases, the samples can be divided basically into six types of minerals: anhydrite, aragonite, calcite, ettringite, calcium sulfate hemihydrate and gypsum divided into three distinct categories: calcium sulfate phases, carbonate phases and ettringite. The anhydrite and calcium sulfate hemihydrate phases were only present in the 7-day reaction samples.

The samples were refined and some adjustments were made using the Rietveld method. The quantification of each mineral was also done through the method, the results can be seen in table 3 below where each constituent was quantified.

Figure 18. XRD for 1.0% chlorine in ettringite synthesis with mineral indications

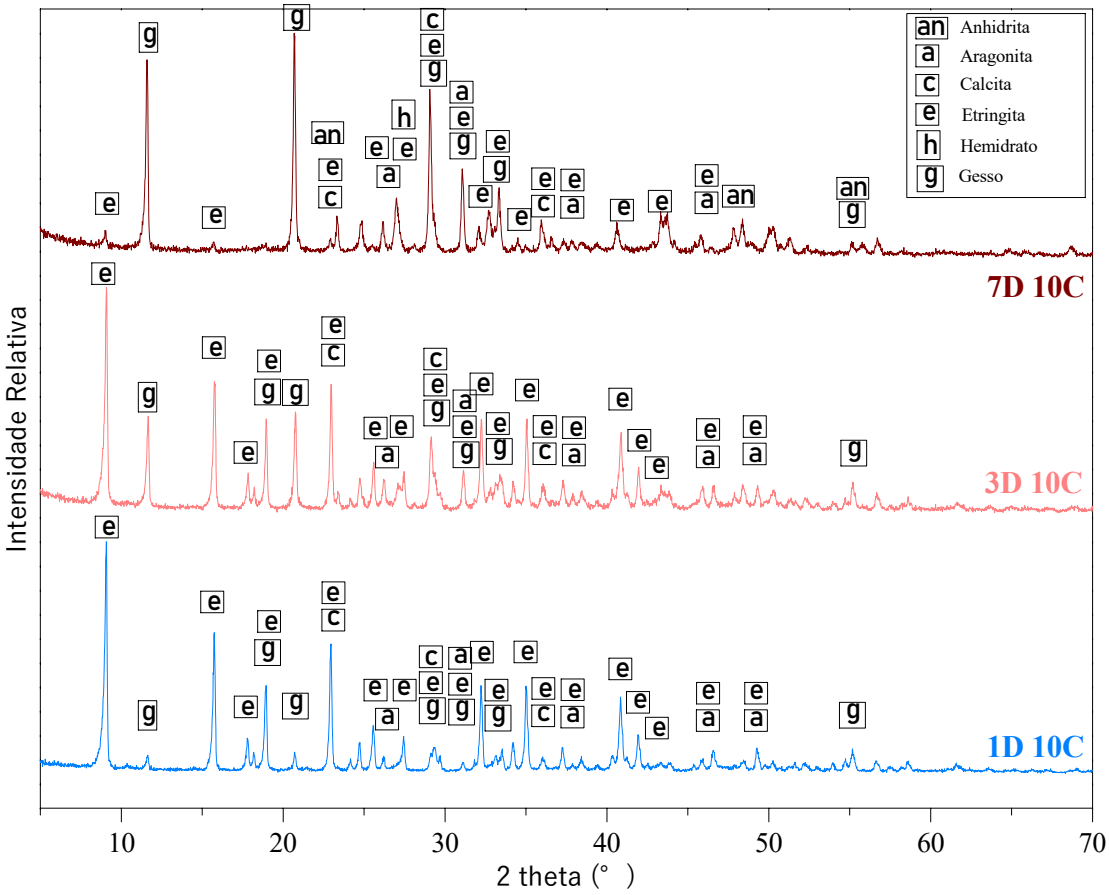


Source: Own authorship.

The unit cell network parameters for each of the samples using the Rietveld method are shown in Table 4 as well as the reference parameters for ettringite present in the scientific literature, in this case represented through the refinement made by (GOETZ-NEUNHOEFFER; NEUBAUER , 2006a).

On the first day of reaction, the main constituent mineral of samples 1D05C, 1D10C and 1D20C was ettringite (GOETZ-NEUNHOEFFER; NEUBAUER, 2006a), it was present in all three samples and varied between 79.58% for the lower concentration, sample 1D05C up to 86.07% for the highest concentration, sample 1D20C. This high concentration of the mineral shows that the result of the synthesis was effective and that the quality standards of the material are satisfactory for experiments and their respective analyses.

The second-highest concentration material was carbonated. Carbonates, as mentioned above, are not expected in the synthesis of ettringite, as they do not exist within the composition of this mineral, as well as carbonates do not exist in the composition of the precursors. However, some of the precursors came with impurities and, in addition, carbonates are formed when the

material comes into contact with the atmosphere containing carbon dioxide. This observation was made even though the synthesis was carried out in the presence of sucrose. Sucrose, in the scientific literature, is capable of inhibiting the effect of carbonate formation (CaCO3). This observation was made by Carlson and Berman when observing the presence of calcite in their research results and to inhibit it, they added sucrose to the mixture (CARLSON; BERMAN, 1960). This same conception was used in these results, but the impediment to the formation of carbonates in the mixture was not observed. This observation is in agreement with KONOPACKA-ŁYSKAWA et al. (2019), he observed in their results that only in the presence of fructose the formation of calcite was slower, therefore, it is recommended to redo the synthesis of ettringite with the application of fructose in place of sucrose.

The third material with the highest concentration was gypsum, which is one of the precursor materials and shows that not all available materials generated ettringite on the first day.

Figure 19. XRD for 2.0% chlorine in ettringite synthesis with mineral indications

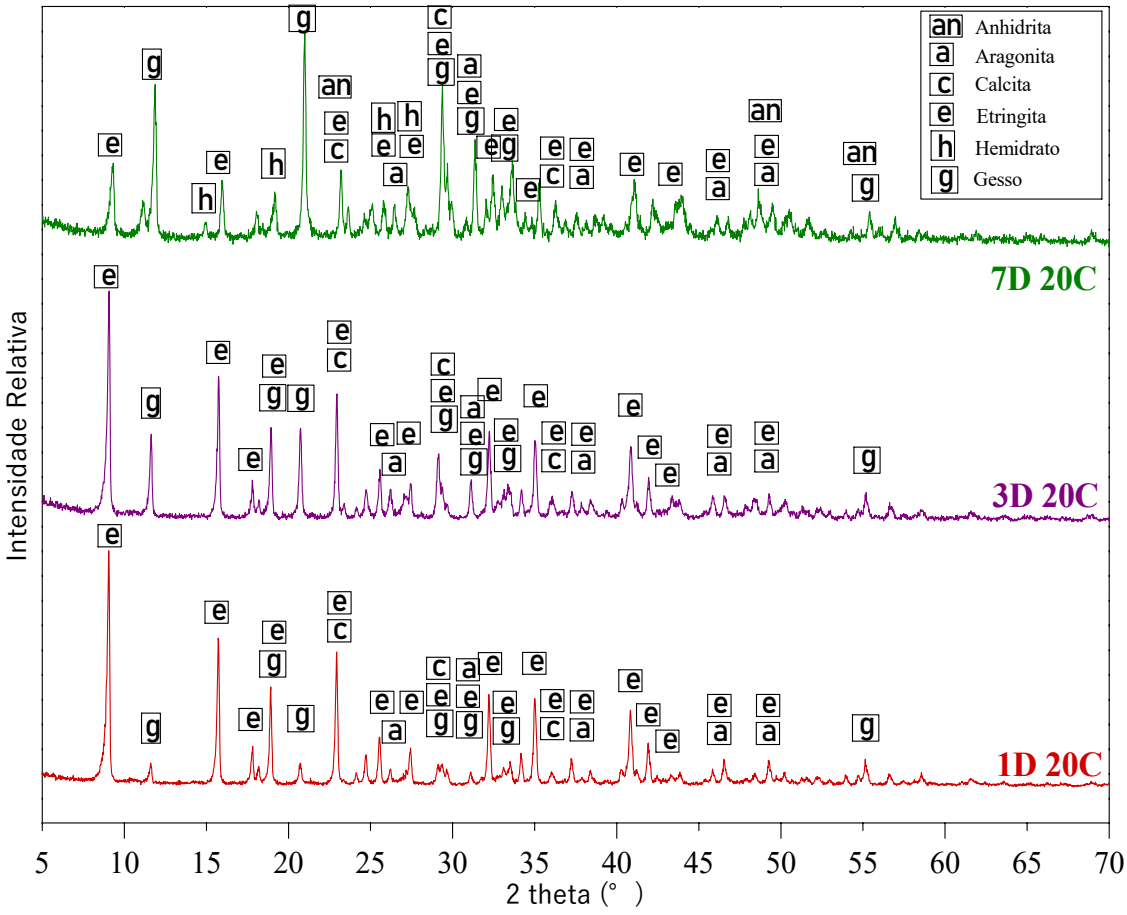


Source: Own authorship.

For the three-day reaction samples, all of them still had ettringite as their major constituent, but in a lower percentage than the one-day reaction samples. The sample, 3D05C, with the highest percentage of ettringite had 89.16%, while the sample, 3D10C, with the lowest percentage, had 64.78%. This trend continued for samples with seven days of reaction with a higher proportion and ranged from 4.32% in the sample with the lowest proportion, 7d10C, to 31.22% for the highest concentration, 7D20C. This decrease may show the effectiveness of chlorine's role in the destruction of ettringite.

Table 3. Quantification of each mineral for each sample using the Rietveld method (%)

| Sample | Ettringite | Gypsym | Aragonite | Calcite | Hemidrate | Anhydrite |
|---|---|---|---|---|---|---|
| **1D 05C** | 79,58 | 9,1 | 7,93 | 3,38 | - | - |
| **1D 10C** | 85,96 | 4,75 | 5,22 | 4,07 | - | - |
| **1D 20C** | 86,07 | 6,32 | 5,63 | 1,98 | - | - |
| **3D 05C** | 89,16 | 3,56 | 5,06 | 2,22 | - | - |
| **3D 10C** | 64,78 | 20,95 | 11,09 | 3,17 | - | - |
| **3D 20C** | 66,15 | 19,58 | 11,26 | 3 | - | - |
| **7D 05C** | 5,71 | 14,02 | 33,83 | 10,86 | 23,53 | 12,05 |
| **7D 10C** | 4,32 | 66,56 | 21,15 | 4 | - | 3,96 |
| **7D 20C** | 31,22 | 45,61 | 11,96 | 4,36 | 4,84 | 2 |

Source: Own authorship.

Comparing the structural refinement of the samples with the refinement of reference of the scientific community, in this case represented by the sample of Neubauer (2006), it is possible to observe that all samples presented parameters affected by the addition of chlorine in their composition. It is possible to observe that with the addition of chlorine in the synthesis all the parameters showed changes. In the direction a, for all samples, there was a considerable expansion, while for the parameter c, a narrowing was observed. For all samples, the parameter a are very similar and there is not a considerable distinction between the samples, so the variation of the chlorine concentration in the synthesis does not influence this parameter so much.

The opposite is observed for parameter c, as samples with seven days of reaction have a reduction in the unit cell in this direction. A slight reduction is also observed when there is an increase in the concentration of chlorine in the samples. The volume of the samples showed a

reduction in volume when compared to the reference sample, in addition the samples suffered a volume reduction as the synthesis developed up to seven days.

Table 4. Structural refinement of each sample using the Rietveld method.

| Sample | *a* | *c* | Volume (Å$^3$) | a/c |
|---|---|---|---|---|
| **Neubauer (2006)** | 11,2290 | 21,478 | 2345,46000 | 0,522814 |
| **1D 05C** | 11,24334 | 21,37159 | 2339,68872 | 0,526088 |
| **1D 10C** | 11,24918 | 21,37025 | 2341,9744 | 0,5263945 |
| **1D 20C** | 11,25085 | 21,36143 | 2341,70068 | 0,5266898 |
| **3D 05C** | 11,24416 | 21,37621 | 2340,53661 | 0,5260129 |
| **3D 10C** | 11,25111 | 21,36419 | 2342,11452 | 0,5266343 |
| **3D 20C** | 11,24763 | 21,3616 | 2340,38192 | 0,5265352 |
| **7D 05C** | 11,24841 | 21,30855 | 2334,89044 | 0,5278822 |
| **7D 10C** | 11,24142 | 21,3459 | 2336,08009 | 0,5266316 |
| **7D 20C** | 11,24964 | 21,3262 | 2337,33851 | 0,5275034 |

Source: Own authorship.

In figure 20 below, the a/c graph of the studied samples was plotted and which are exposed above in table 4, they were differentiated by colored balls, where the blue ones were samples with 0.5% chlorine in their composition, see samples with 1.0% and red samples with 2.0%. The size of the circles was differentiated by the concentration of ettringite, where samples with a higher concentration of ettringite in their composition have larger circles and samples with a lower concentration of ettringite are presented in smaller circles. The “end members” were also exposed in the graphic and they were linked to each other. These two points represent thaumasite (lowest Δ point) and ettringite (highest Δ point) in their pure states. Also exposed in the graph, are samples of ettringite from other researchers with different modifications. Norman et al. (2013), for example, present aluminum, manganese, gallium, iron or tin. On the other hand, the Hartman samples; Berliner (2006) show a different chemical composition even though they have the same precursor elements ($Ca_6[Al(OH)_6]_2(SO_4)_3 \cdot 26H_2O$). Some researchers have made more than one change in the chemical composition of ettringite. Two of them are shown in figure 20 below: Norman et al. and those of Poellmann. This decision was made to analyze the influence of the presence of a different chemical element on its composition. In addition, the radius of each of these cations was placed.

Figure 20. a versus c for samples with 0.5, 1.0 and 2.0% chlorine (O) concentration together with samples of ettringite synthesis from other authors.

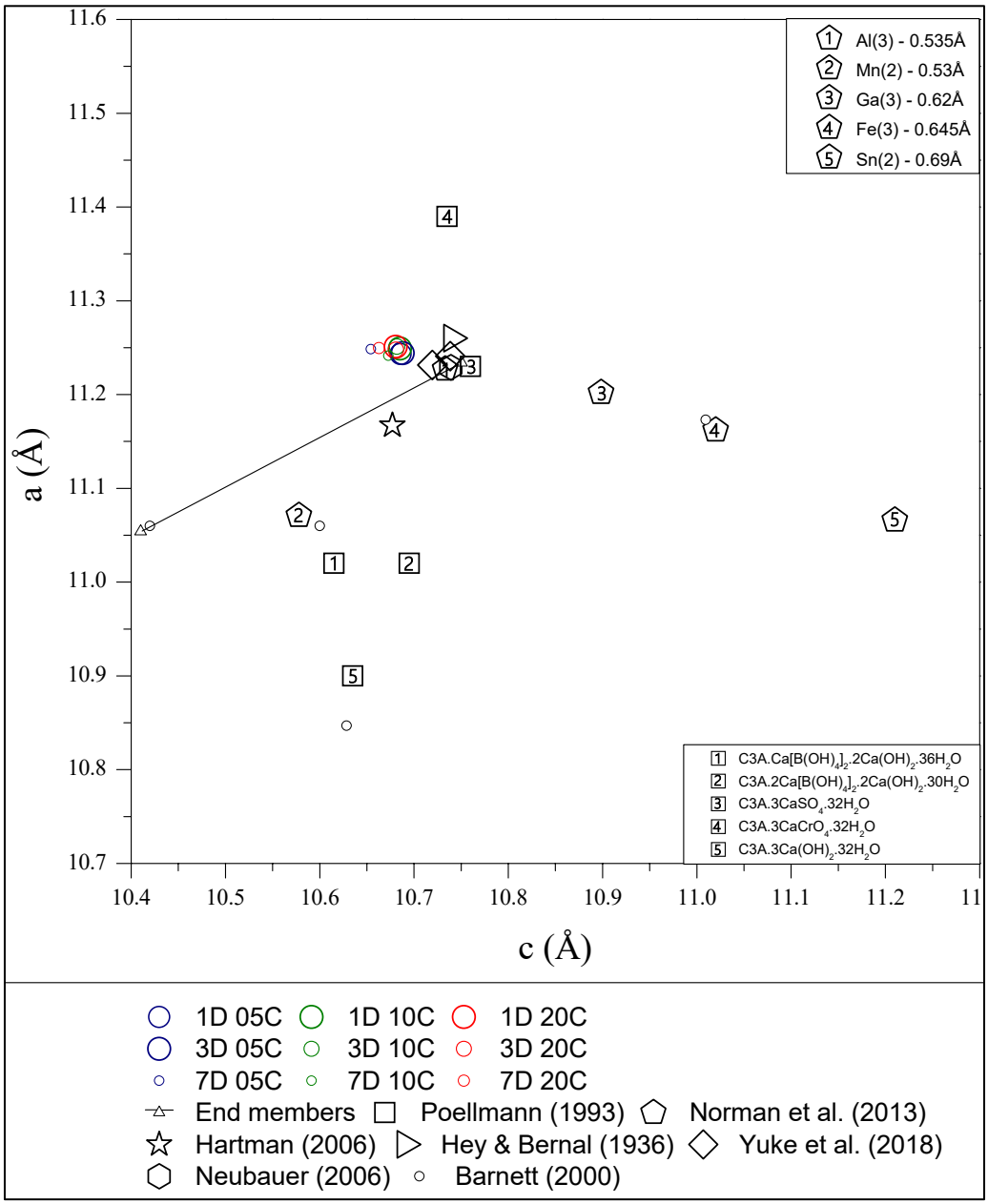


Source: Own authorship.

By observing the samples studied by this experiment, it is possible to observe, firstly, that the samples are closer to pure ettringite than pure thaumasite, in addition, it is possible to observe that all samples presented a shift to the left in the graph. This shows that the length of parameter c decreased, whereas the length of parameter a remained almost constant. Therefore, the presence of chlorine in the composition of ettringite mainly influences the c of the crystal structure.

## 3.5 Thermal Analysis

The heat flux, mass loss and mass derivative results for all nine samples are shown below in figure 26. In these figures each result was plotted on individual curves in a triple y plot, where the heat flux results were differentiated by the green color, the mass loss results were displayed in the blue color and the mass derivative results were differentiated by the red color.

The phases were previously identified before the thermal analysis through the XRD test, already exposed in this work. In all nine ettringite samples a high endothermic peak between 90ºC and 100ºC and another between 120ºC and 150ºC was identified in the graph of the mass derivative corresponding to the decomposition of ettringite, followed by another endothermic peak, a little lower, between 240ºC and 250ºC corresponding to the gypsum peak. After a long period without any considerable change in the graph, the endothermic curve for amorphous calcium carbonate appears in a range between 530ºC and 550ºC. Soon after, a medium endothermic peak of aragonite appears. The last peak is low, is also endothermic and is between 850ºC and 890ºC and refers to calcite.

From a thermogravimetric analysis and evaluating the value of mass loss that occurred between the temperatures of each peak, it was possible to determine the content of each of the minerals and their participation in each of the samples, as shown in table 5 below.

Table 5. Quantification of each mineral for each sample using the mass loss method (%)

| Sample | Ettringite | Gypsum | Amorphous carbo. | Aragonite | Calcite | Hemydrate |
|---|---|---|---|---|---|---|
| **1D 05C** | 53,80 | 28,85 | 5,42 | 10,46 | 1,47 | |
| **1D 10C** | 55,38 | 29,51 | 5,27 | 8,42 | 1,41 | |
| **1D 20C** | 52,52 | 30,81 | 6,04 | 9,03 | 1,60 | |
| **3D 05C** | 56,52 | 29,04 | 5,07 | 8,16 | 1,20 | |
| **3D 10C** | 46,53 | 32,24 | 6,81 | 12,62 | 1,80 | |
| **3D 20C** | 44,70 | 33,79 | 6,65 | 12,61 | 2,25 | |
| **7D 05C** | 24,81 | 28,63 | 5,81 | 11,07 | 2,64 | 27,04 |
| **7D 10C** | 28,74 | 48,65 | | 20,96 | 1,64 | |
| **7D 20C** | 29,70 | 39,99 | 5,46 | 13,46 | 1,30 | 10,08 |

Source: Own authorship.

It is possible to observe these data exposed below in figure 21, 22 and 23, for the samples that contained 0.5%, 1.0% and 2.0% respectively.

Figure 21. Composition of ettringite with 0.5% chlorine in the synthesis

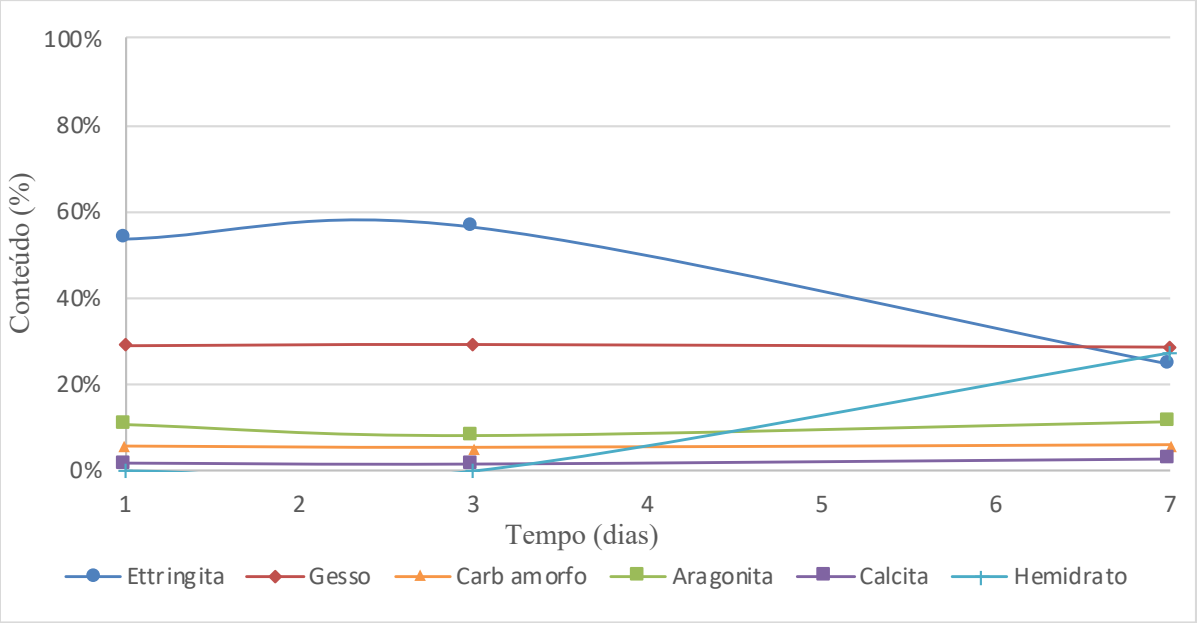


Source: Own authorship.

Figure 22. Composition of ettringite with 1.0% chlorine in the synthesis

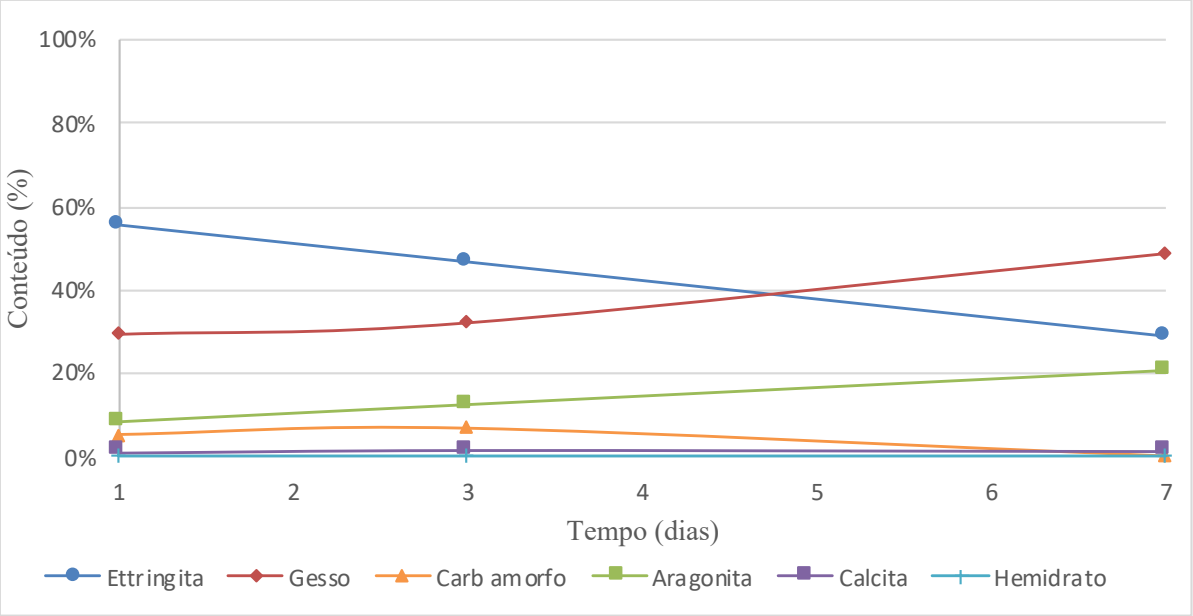


Source: Own authorship.

Figure 23. Composition of ettringite with 2.0% chlorine in the synthesis

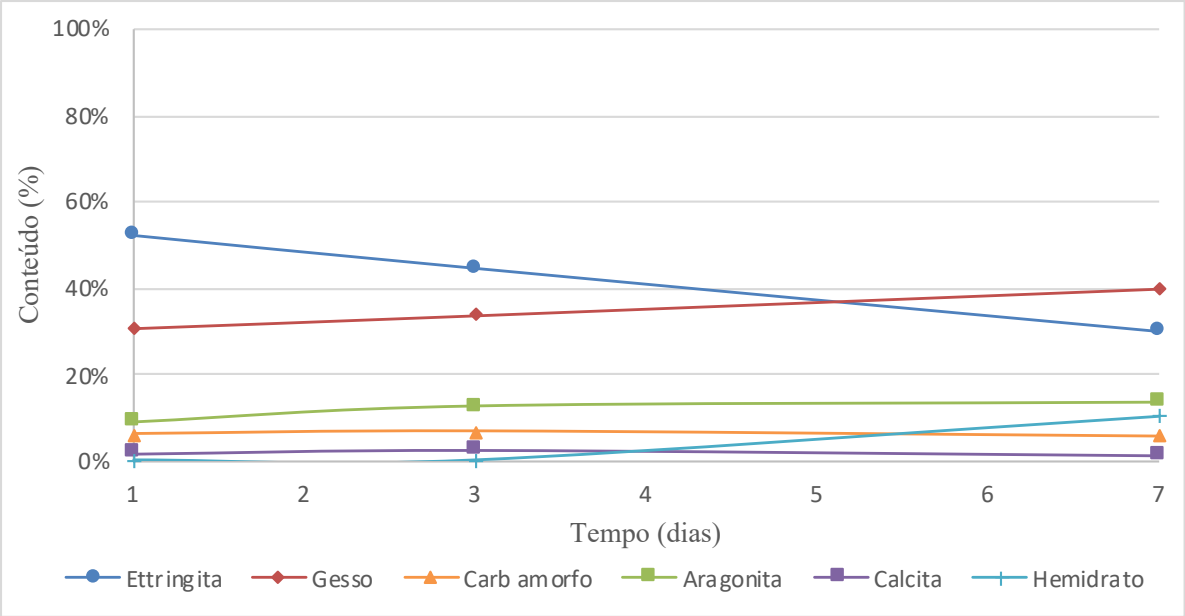


Source: Own authorship.

The figures for 1.0% and 2.0% show that as the reaction developed over time, there was a reduction in the participation of ettringite and an increase in gypsum and hemihydrate. This result indicates that with increasing chlorine in the synthesis, ettringite is likely to be converted to monosulfate or metaettringite over time. As for the 0.5% figure, it showed that there was an increase in the participation of ettringite on the third day of reaction, but this increase was soon overcome as the reaction developed until its seventh day of reaction. A similar result was observed in the XRD test for 0.5% chlorine. The quantification of gypsum remained almost constant. Therefore, it is possible that there is a correlation between the concentration of chlorine in the reaction and the participation of ettringite. As for aragonite, it was possible to observe its increase with time and calcite and amorphous carbonate remained constant for the samples of the three different chlorine concentrations.

When looking at the results of Fridrichová et al. (2018) who synthesized their samples in a similar way to this work, we can see a clear influence of chlorine on the concentrations of each content of the samples. While in Fridrichová's results ettringite is always followed by gypsum and carbonates, in the three results of this research gypsum exceeded the concentration of ettringite. In addition, the decomposition of ettringite led to an increase in the concentration of carbonates over time, whereas in Fridrichová's results there was a reduction in the concentration of carbonates.

In Figure 24 below, the results of the XRD test were compared with the DTA test. On the X axis, the concentration of each of the minerals was exposed for the DTA test, on the Y

axis, the results were exposed in the same reaction time for the XRD test. Therefore, the closer the points were to the 45oC line in the center of the graph, the more similar these results are, the further away from the reference line, the more these results differ from each other.

Figure 24. XRD versus DTA for each compound

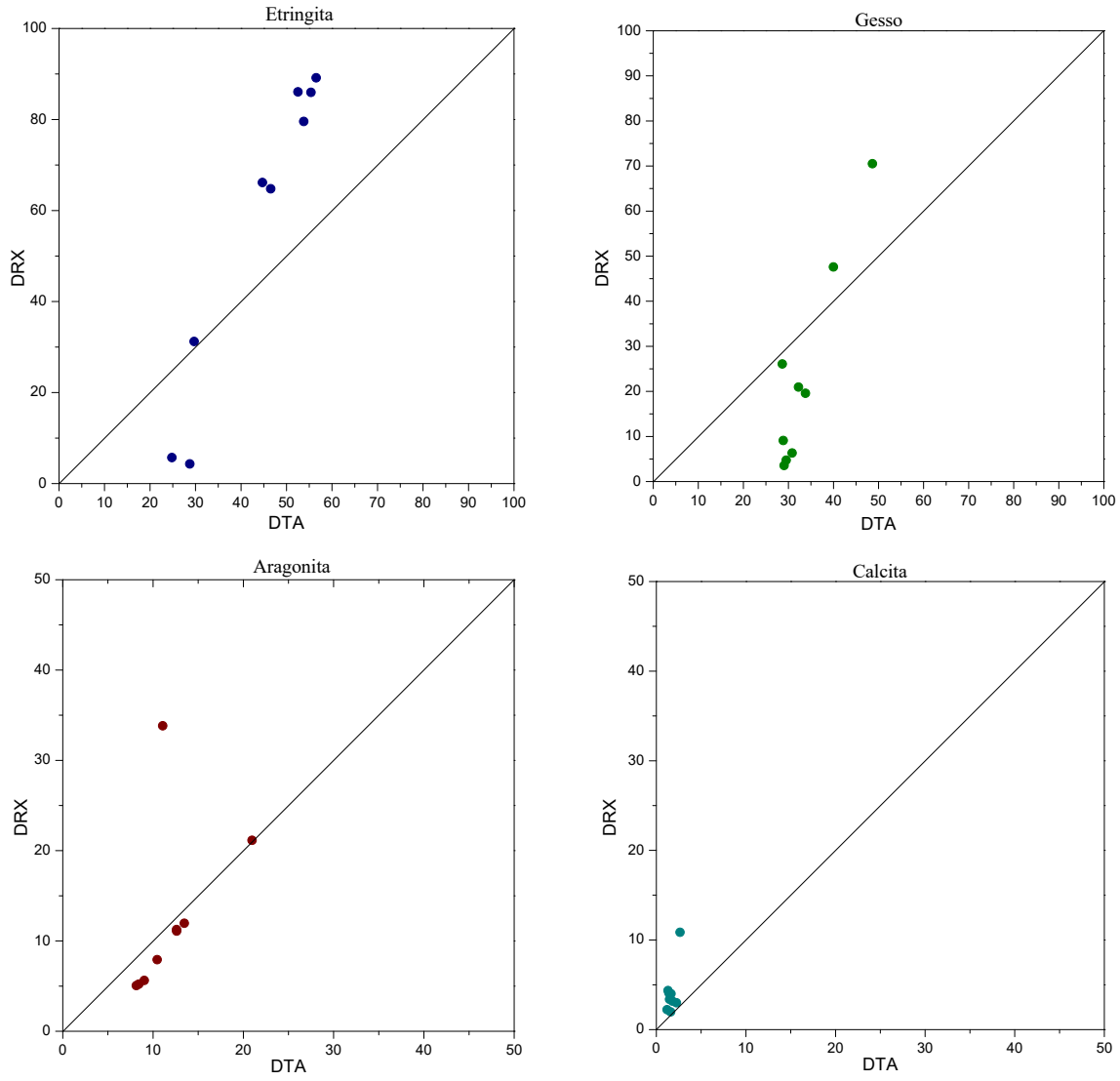


Source: Own authorship.

With these results, it was possible to observe that for both aragonite and calcite, the results of XRD and DTA were very close. This certifies that both methods are important for sample characterization, as both carbonates are crystalline and can be identified by the diffraction method. However, the DTA method stands out in carbonates compared to the XRD method, because in addition to the precise identification of crystalline carbonates, it was also possible to quantify amorphous carbonates. Only one result differed between the two methods and for both the differentiation occurred for the result of seven days of reaction with 0.5%

chlorine in its composition. This same difference was observed for both sulfates and ettringite. When analyzing the diffractogram of this sample, we see that it presents a lot of noise characteristic of amorphous material, so this may be one of the reasons why this sample differed so much between both experiments since the XRD is not the most suitable method for characterization and quantification of materials. amorphous.

As for gypsum and ettringite, although the XRD and DTA results follow the same trend, depending on the chlorine concentration and reaction time, there is a considerable difference between the results, but if we add the values of ettringite and gypsum for the same concentration of chlorine and for the same reaction time, as shown in Figure 25 below, we can see that the values of XRD and DTA are considerably similar.

Figure 25. XRD versus DTA for sum of ettringite and calcium sulfates

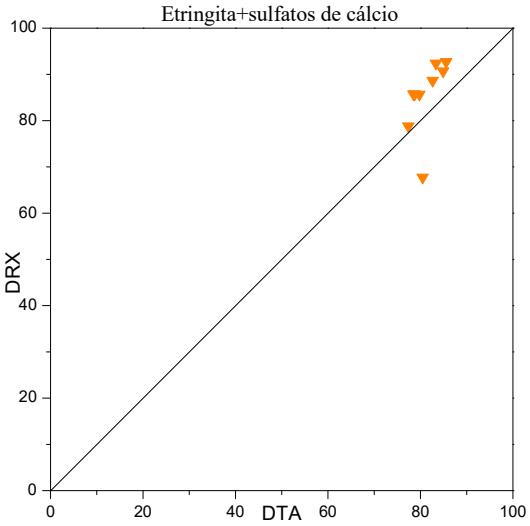


Source: Own authorship.

There are two explanations for this situation. The first is that XRD is much more capable of separating ettringite and gypsum than TGA, in situations where the crystallinity of the phases is still preserved. The peaks of these minerals are quite distinct in the diffractogram. In TGA, the separation of the loss of water molecules in both minerals is very close and sometimes they overlap, especially when the crystallinity of the minerals is affected. There is an overlap around the 150oC peak, making it difficult to obtain an exact result for both minerals. The second explanation is that both ettringite and sulfates can have low degree of crystallinity and, for this situation, XRD cannot fully quantify the minerals. It is interesting to note that the sample that most deviates from the 45ºC line is the same sample that differed from the other samples for calcite and aragonite and the explanation for this differentiation is the same.

Figure 26. Individual thermogravimetry, heat flux and mass derivative of all samples

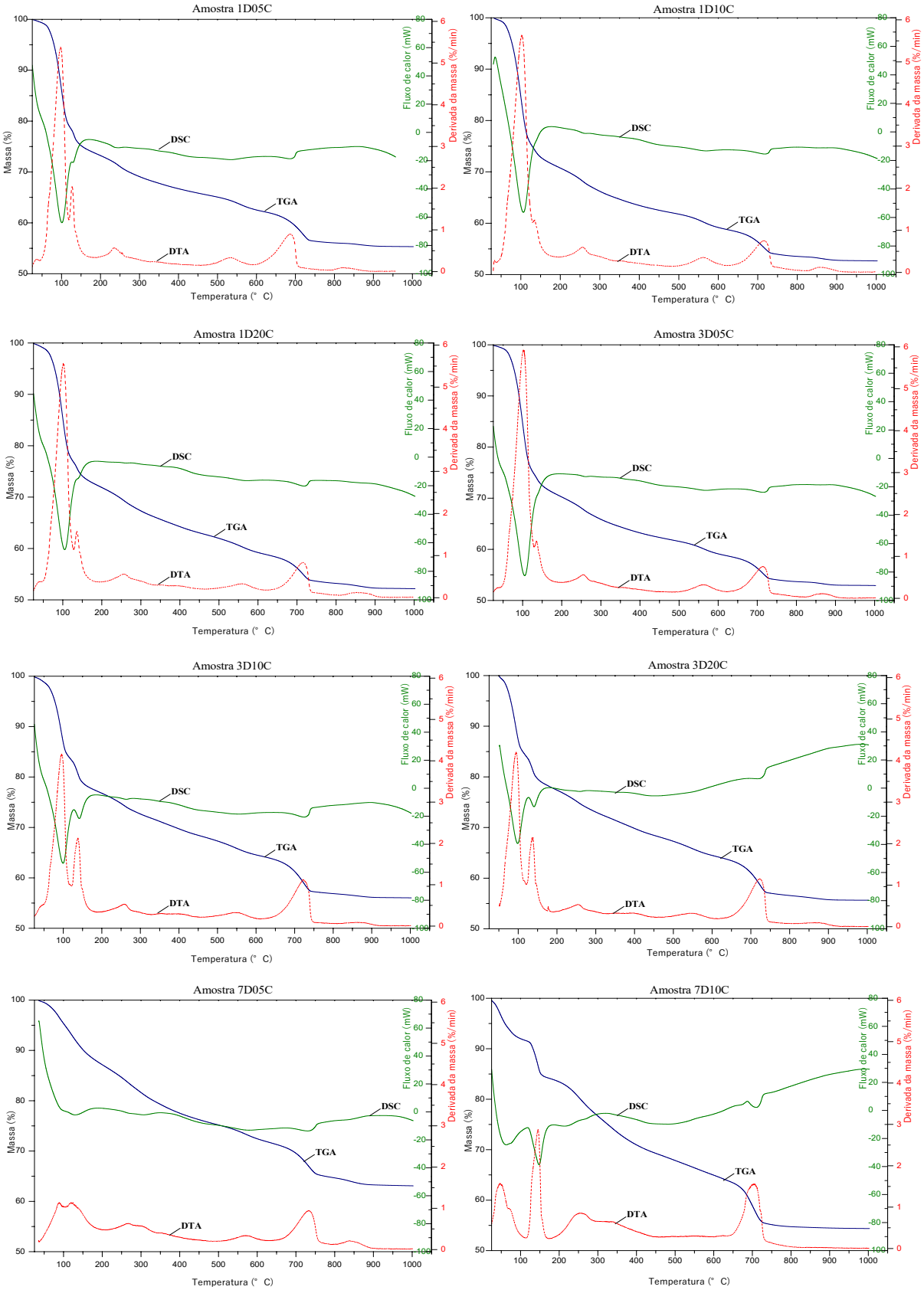

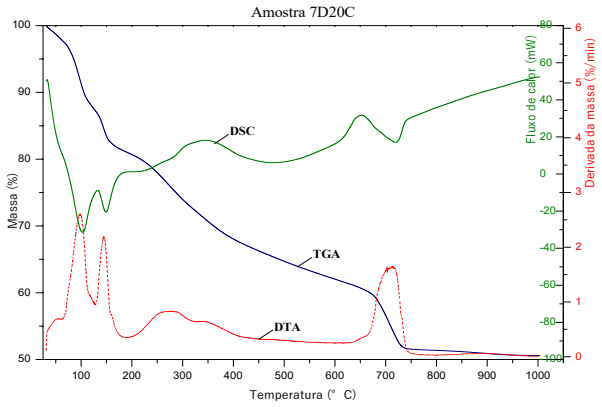


Source: Own authorship.

In general, the thermal analysis was fundamental to provide important knowledge about the role of chlorine in the synthesis of ettringite. It showed the deterioration of ettringite over time and, on the other hand, the formation of gypsum and carbonates in the samples. It showed that as chlorine was increased, this relationship became more evident.

## 3.6 Scanning Electron Microscopy

All nine types of ettringite samples were analyzed in SEM. A small representative part of each of them was chosen and the scanning electron microscopy test was carried out. The images were taken with the objective of a better visualization of the phases of the sample and, through that, a better understanding of each one of them, in addition, to look for some differences that by chance could appear between them.

The images were taken at three different magnitudes: 5000x, 10000x and 25000x magnification of various regions of the sample. Being posted in this work only the most representative images that exhibit some characteristic phase, such as ettringite, gypsum and carbonates. In figures 27, 28 and 29, the images with only 1 day of reaction and with 10000x and 25000x of magnitude are represented, whereas in figures 30, 31 and 32 the images with 3 days of reaction and with 10000x and 25000x of magnitude are represented, Figures 33, 34 and 35 represent the images with 7 days of reaction and with 5000x, 10000x and 25000x of magnitude.

Green rectangles were used to highlight the presence of the thin, long and hexagonal needle-shaped crystals of the ettringite. For the gypsum prismatic crystals, orange rectangles were used. The carbonate crystals, on the other hand, are much larger than the ettringite and

gypsum crystals and present morphology closer to the orthorhombic and were distinguished by the blue color.

Figure 27. SEM images of sample 1D05C with a) 10000x, b) 25000x magnitude.

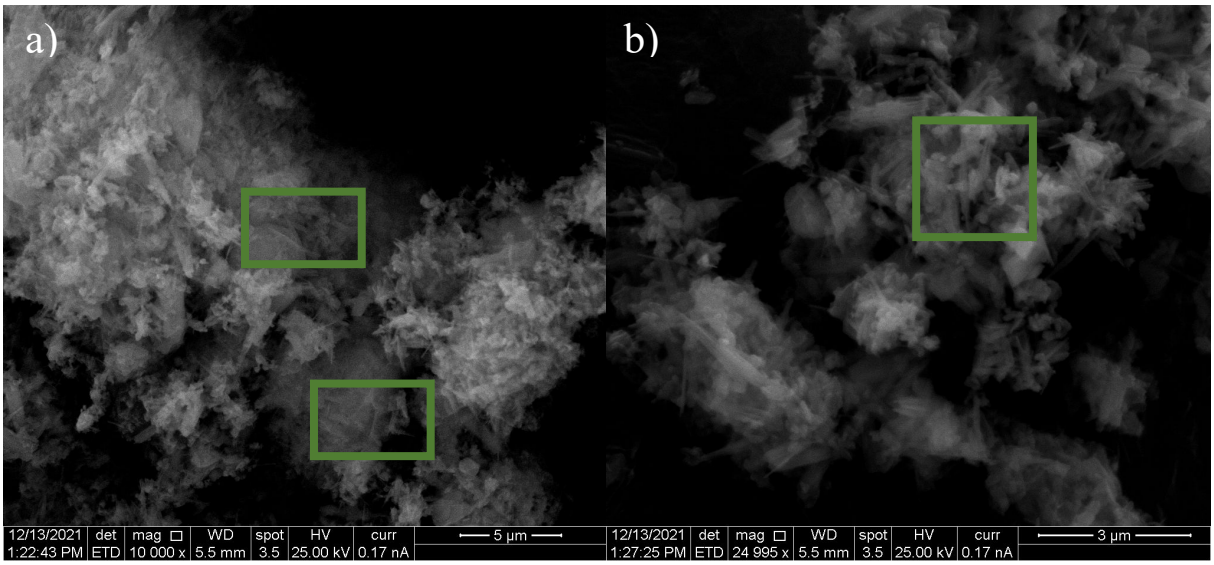


Source: Own authorship.

In figures 27, 28, 29 and 30 it is possible to observe the large presence of fine and long needles characteristic of ettringite. These needles were in large quantities throughout the sample, thus facilitating the acquisition of images of the same.

Figure 28. SEM images of sample 1D10C with a) 10000x, b) 25000x magnitude.

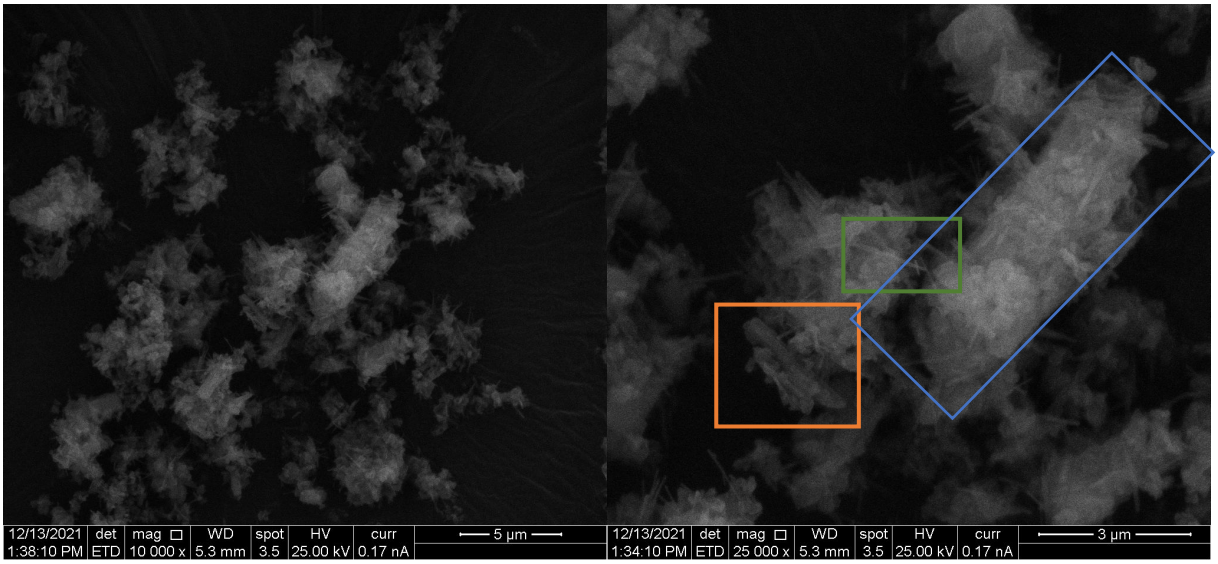


Source: Own authorship.

It was also possible to easily find gypsum crystals throughout the sample. Gypsum crystals have a more prismatic character than ettringite needles and are not as thin and long. They appear in the form of long, prismatic rods.

Figure 29. SEM images of sample 1D20C with a) 10000x, b) 25000x magnitude.

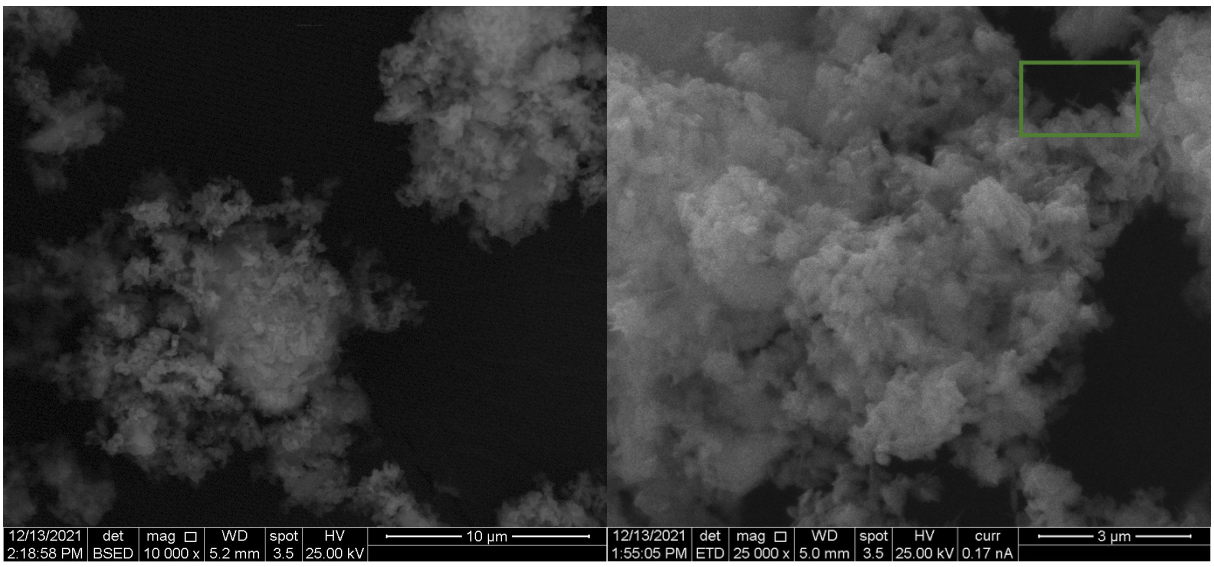


Source: Own authorship.

It was also possible to find carbonate crystals in the sample. The carbonate crystals are much larger than the thin, elongated crystals of ettringite and the elongated, prismatic crystals of gypsum.

Figure 30. SEM images of sample 3D05C with a) 10000x, b) 25000x magnitude

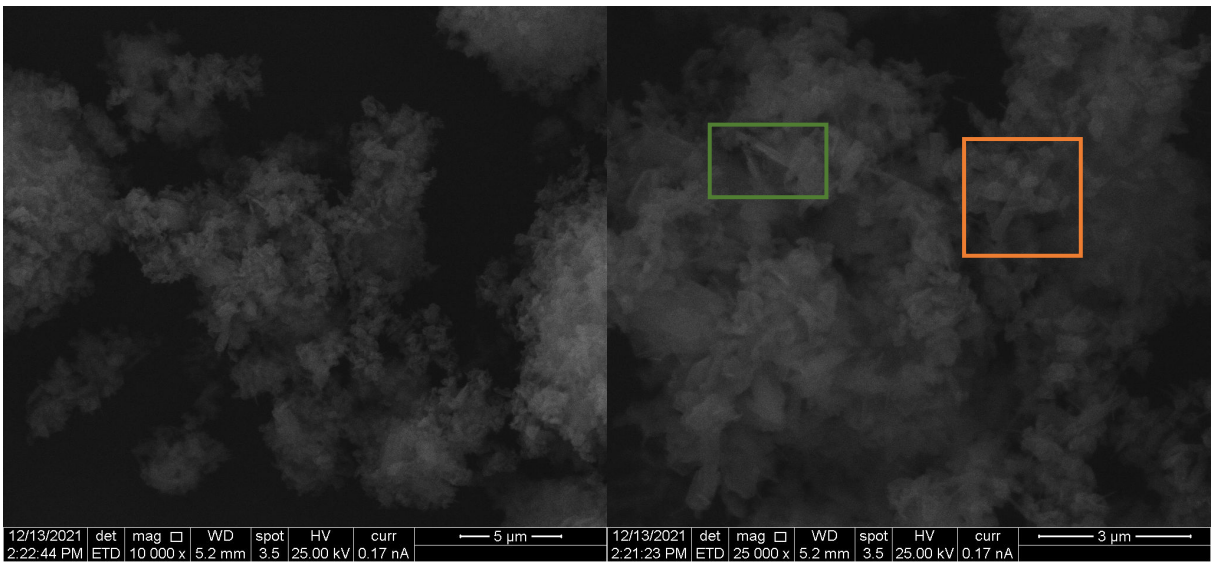


Source: Own authorship.

In figures 31 and 32, it is already more difficult to visualize the thin and elongated needles characteristic of ettringite when compared to the previous samples, but it is still the most present morphology in the samples along with the gypsum crystals. It is also possible to observe more frequent carbonates in the images.

Figure 31. SEM images of sample 3D10C with a) 10000x, b) 25000x magnitude

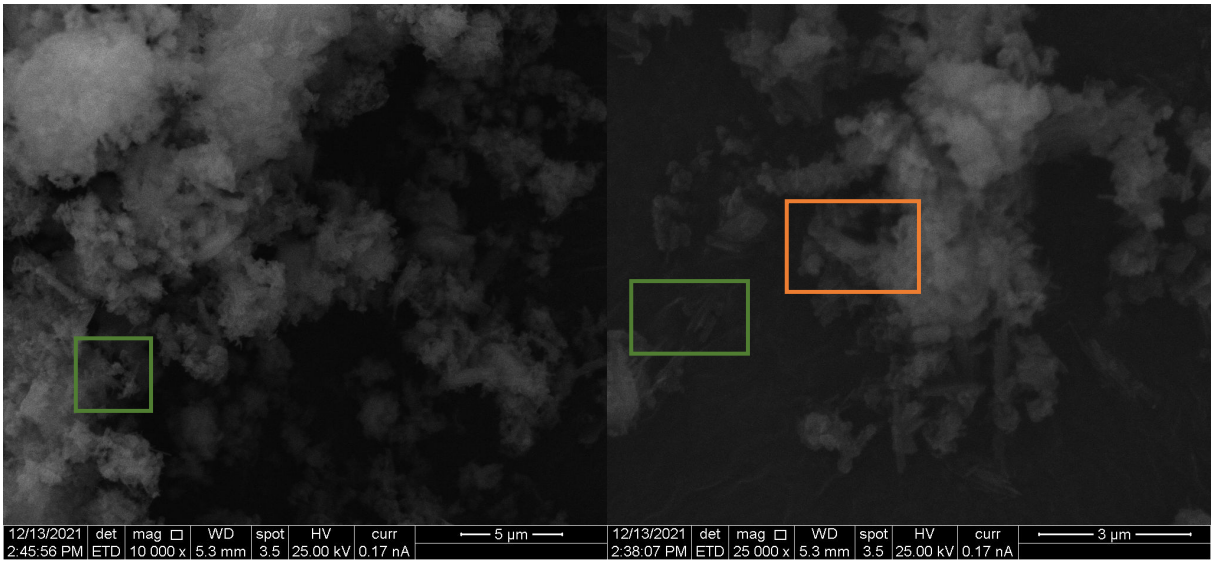


Source: Own authorship.

Figure 32. SEM images of sample 3D20C with a) 10000x, b) 25000x magnitude

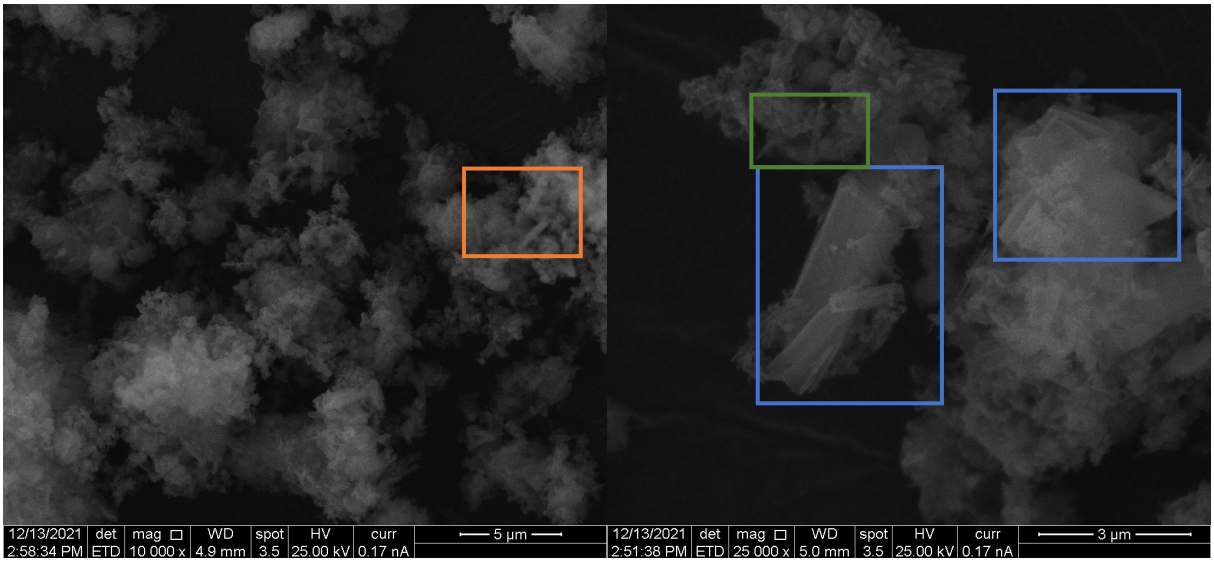


Source: Own authorship.

In figures 33, 34 and 35, it is very difficult to observe ettringite, the crystals in these images are larger than those observed in the previous figures. It is easier to observe gypsum crystals and carbonates.

Figure 33. SEM images of sample 7D05C with a) 10000x, b) 25000x magnitude

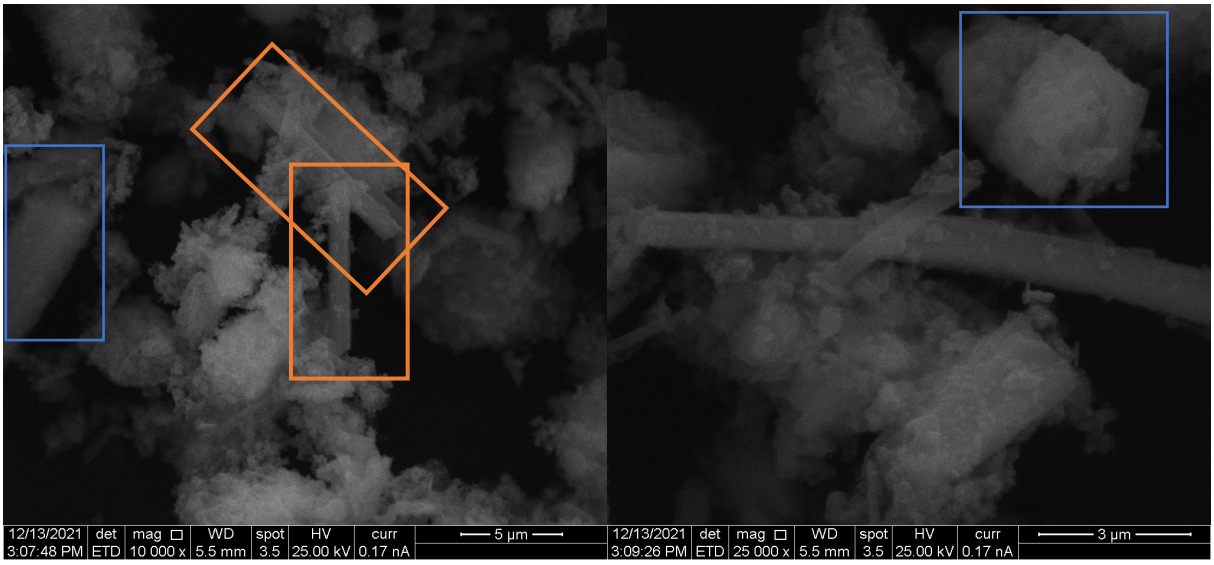


Source: Own authorship.

Because the carbonate crystals are larger than the ettringite and gypsum crystals, the images with 10000x magnitude did not show the crystals with quality, so for these images a magnitude of 5000x was used. It is quite evident in the images a greater presence of carbonate crystals.

Figure 34. SEM images of sample 7D10C with a) 5000x, b) 25000x magnitude

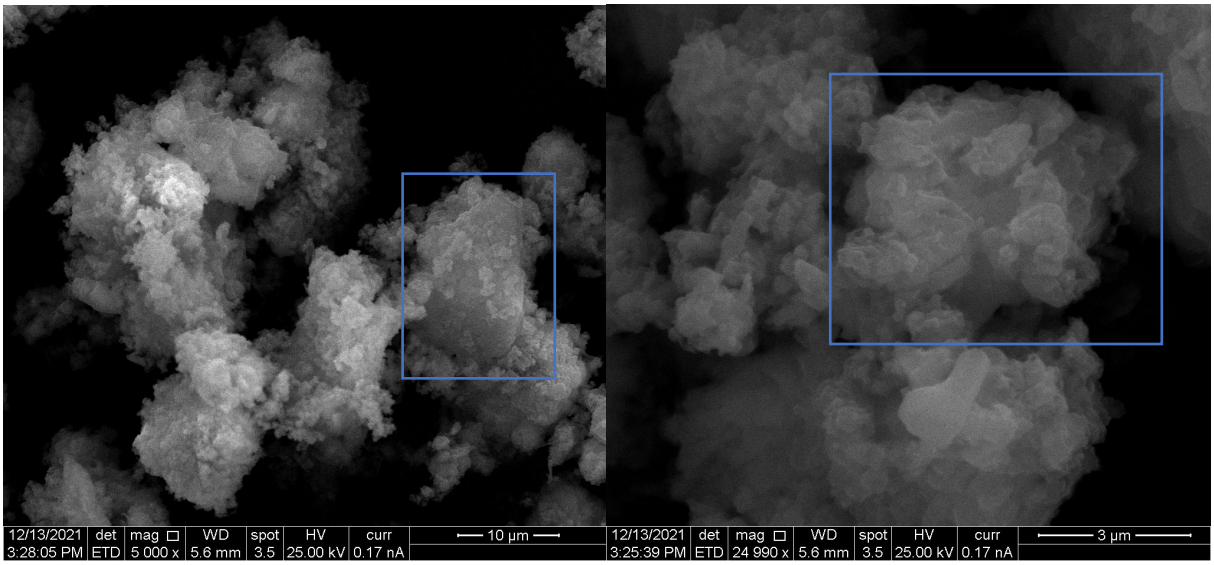


Source: Own authorship.

Figure 35. SEM images of sample 7D20C with a) 5000x, b) 25000x magnitude

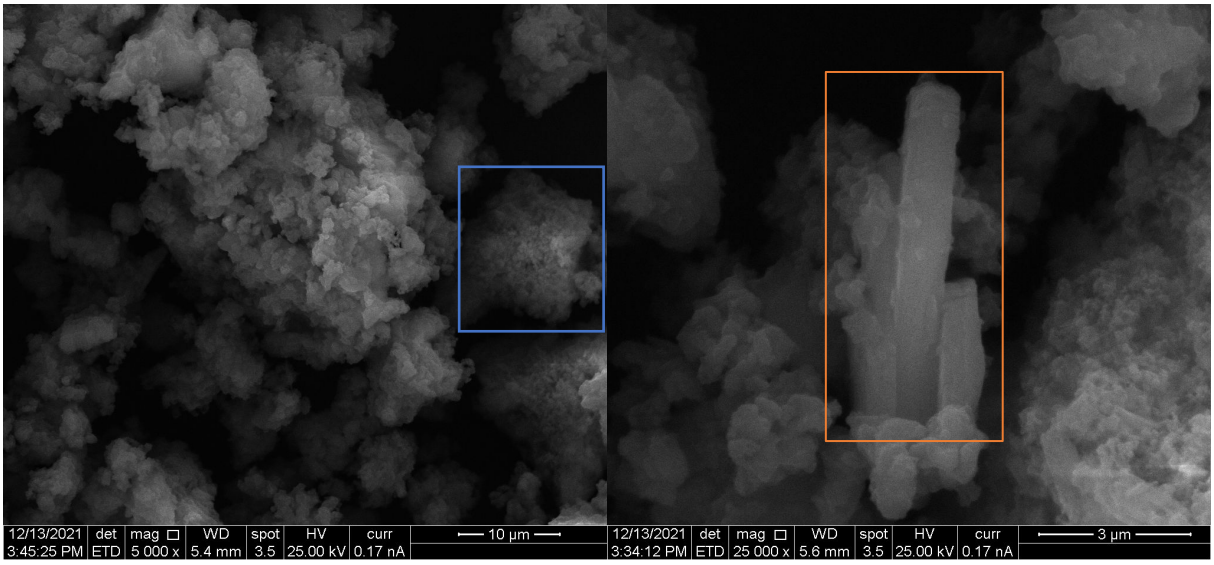


Source: Own authorship.

# 4 CONCLUSION

Due to the increasing number of occurrences of structures affected by late ettringite, it is interesting to encourage and search for answers that prevent its emergence, since although there are very few definitive corrective solutions, it is possible to prevent new structures from manifesting this pathology using methods effective in prevention. The synthesis of this mineral helped to facilitate the study as well as to replace some constituent elements with different ions.

It was possible to observe through this dissertation the possibility of artificially generating ettringite through simple means and products that are easy to find, in addition, the synthesis of ettringite was successful and chlorine was adsorbed on its structure. It was also possible to observe that the presence of chlorine in the ettringite mineral represents a change in the lengths of the structural parameters a and c of the mineral and that the greater the percentage of chlorine in the structure, the greater the stabilization of ettringite and that with the increase of chlorine in the synthesis, ettringite is likely to be converted to monosulfate or metaettringite over time.

For future work, it is proposed to continue the investigation of the influence of chlorine on the stabilization of ettringite through a greater variation in its concentration. In addition, further investigation is proposed through the EDS test at random points of the physical sample since in terms of characterization techniques, XRD and SEM/EDS are essential for a good implementation of the quantitative analysis of Rietveld Refinement.

**REFERENCES**


ABRAHAM, J. et al. Chapter 8 - Thermoanalytical Techniques of Nanomaterials. In: MOHAN BHAGYARAJ, S. et al. (Eds.). . **Characterization of Nanomaterials**. [s.l.] Woodhead Publishing, 2018. p. 213–236.

ÁLVAREZ-AYUSO, E.; NUGTEREN, H. W. Synthesis of ettringite: A way to deal with the acid wastewaters of aluminum anodizing industry. **Water Research**, v. 39, n. 1, p. 65–72, 2005.

BAQUERIZO, L. G. et al. Hydration states of AFm cement phases. **Cement and Concrete Research**, v. 73, p. 143–157, 2015.

BENSTED, J.; RBROUGH, A.; PAGE, M. M. 4 - Chemical degradation of concrete. In: PAGE, C. L.; PAGE, M. M. (Eds.). . **Durability of Concrete and Cement Composites**. [s.l.] Woodhead Publishing, 2007. p. 86–135.

CARLSON, E. T.; BERMAN, H. A. **Some Observations on the Calcium Aluminate Carbonate HydratesJOURNAL OF RESEARCH of the National Bureau of Standards-A. Physics and Chemistry**. [s.l: s.n.].

CHATTERJEE, A. K. 8 - X-Ray Diffraction. In: RAMACHANDRAN, V. S.; BEAUDOIN, J. J. (Eds.). . **Handbook of Analytical Techniques in Concrete Science and Technology**. Norwich, NY: William Andrew Publishing, 2001. p. 275–332.

COLLEPARDI, M. **A state-of-the-art review on delayed ettringite attack on concrete Cement and Concrete Composites** Elsevier Ltd, , 2003.

EKOLU, S. O. Influence of Synthetic Zeolite on Delayed Ettringite Formation – Preliminary Investigation. **ACI Symposium Publication**, v. 326, 2018.

EKOLU, S.; THOMAS, M. D. A.; HOOTON, D. Pessimum effect of externally applied chlorides on expansion due to delayed ettringite formation: Proposed mechanism. **Cement and Concrete Research**, v. 36, p. 688–696, 15 abr. 2006.

FRIDRICHOVÁ, M. et al. **Synthetic preparation and properties of ettringite**. Key Engineering Materials. **Anais**...Trans Tech Publications Ltd, 2018.

GOETZ-NEUNHOEFFER, F.; NEUBAUER, J. Refined ettringite (Ca6Al2(SO4)3(OH)12·26H2O) structure for quantitative X-ray diffraction analysis. **Powder Diffraction**, v. 21, n. 1, p. 4–11, 2006a.

GOETZ-NEUNHOEFFER, F.; NEUBAUER, J. Refined ettringite (Ca 6 Al 2 (SO 4 ) 3 (OH) 12 ·26H 2 O) structure for quantitative X-ray diffraction analysis . **Powder Diffraction**, v. 21, n. 1, p. 4–11, mar. 2006b.

**Handbook of Mineralogy**.

HARTMAN, M. R.; BERLINER, R. Investigation of the structure of ettringite by time-of-flight neutron powder diffraction techniques. **Cement and Concrete Research**, v. 36, n. 2, p. 364–370, fev. 2006.

HOU, D. et al. Insight on the sodium and chloride ions adsorption mechanism on the ettringite crystal: Structure, dynamics and interfacial interaction. **Computational Materials Science**, v. 153, p. 479–492, 1 out. 2018.

ICTA. **For Better Thermal Analysis and Calorimetry**. 3. ed. [s.l.] International Confederation for Thermal Analysis, 1991, 1991.

KONOPACKA-ŁYSKAWA, D. et al. Influence of selected saccharides on the precipitation of calcium-vaterite mixtures by the CO 2 bubbling method. **Crystals**, v. 9, n. 2, 1 fev. 2019.

L. PAVIA, D.; M. LAMPMAN, G. **Introdução à Espectroscopia**. 5ª Edição ed. [s.l.] Cegage, 2016.

MARTÍNEZ-RAMÍREZ, S. et al. In-situ reaction of the very early hydration of C3A-gypsum-sucrose system by Micro-Raman spectroscopy. **Cement and Concrete Composites**, v. 73, p. 251–256, 1 out. 2016.

MONTEIRO, P. J. M.; P. MEHTA. Concrete - Microstructure Properties and Materials. **McGraw Hill professional**, v. 3, p. 0–659, 2005.

MORANVILLE-REGOURD, M.; KAMALI-BERNARD, S. 10 - Cement Made From Blast furnace Slag. In: HEWLETT, P. C.; LISKA, M. (Eds.). . **Lea's Chemistry of Cement and Concrete (Fifth Edition)**. [s.l.] Butterworth-Heinemann, 2019. p. 469–507.

NAKAMOTO, K. **Infrared and Raman Spectra of Inorganic and Coordination Compounds**. 6th edition ed. [s.l: s.n.].

NORMAN, R. L. et al. Synthesis and structural characterization of new ettringite and thaumasite type phases: Ca6[Ga(OH)6·12H2O] 2(SO4)3·2H2O and Ca 6[M(OH)6·12H2O]2(SO 4)2(CO3)2, M = Mn, Sn. Solid-State **Sciences**, v. 25, p. 110–117, 2013.

ODLER, I.; ABDUL-MAULA, S. **POSSIBILITIES OF QUANTITATIVE DETERMINATION OF THE AFt-(ETTRINGITE) AND AFm-(MONOSULPHATE) PHASES IN HYDRATED CEMENT PASTESCEMENT and CONCRETE RESEARCH**. [s.l: s.n.].

OZAWA, T. **Thermal analysis - review and prospect**. [s.l: s.n.].
POELLMANN, H. et al. **SOLID SOLUTION OF ETTRINGITES PART II: INCORPORATION OF B(OH) 4-AND CrO42-IN 3CaO-AI203"3CaSO4"32H20CEMENT and CONCRETE RESEARCH**. [s.l: s.n.].

PÖLLMANN, H.; KUZEL, H.-J.; WENDA, R. Compounds with ettringite structure. **N. Jb. Miner. Abh.**, v. 160, p. 133–158, 1 jan. 1989.

LAVINSKY, R. (2020), fotografia retirada do site iRocks.com

SARGENT, P. 21 - The development of alkali-activated mixtures for soil stabilization. In: PACHECO-TORGAL, F. et al. (Eds.). . **Handbook of Alkali-Activated Cement, Mortars and Concretes**. Oxford: Woodhead Publishing, 2015. p. 555–604.

TELFORD T., CEB Design Guide, Durable Concrete Structures, London (1989)

WARREN, C. J.; REARDON, E. J. **THE SOLUBILITY OF ETTRINGITE AT 25°C**. [s.l: s.n.].

YANG, L. Scanning Electron Microscopy. In: **Materials Characterization**. [s.l.] John Wiley & Sons, Ltd, 2008a. p. 121–144.

YANG, L. X-Ray Diffraction Methods. In: **Materials Characterization**. [s.l.] John Wiley & Sons, Ltd, 2008b. p. 45–77.

YANG, L. X-Ray Spectroscopy for Elemental Analysis. In: **Materials Characterization**. [s.l.] John Wiley & Sons, Ltd, 2008c. p. 171–196.

YUAN, Q. et al. Chapter 2 - Inorganic cementing materials. In: YUAN, Q. et al. (Eds.). . **Civil Engineering Materials**. [s.l.] Elsevier, 2021. p. 17–57.